

(BMI), and postoperative complications.^{9–11} Limitations in these studies, such as unspecified preoperative diabetic status of the patients and inconsistent standards used for the diagnosis of postoperative diabetes, make it difficult to reliably identify risk factors for postoperative diabetes.

Although the mass of pancreatic beta cells has been identified as an important determinant of plasma glucose levels in rodents, dogs, monkeys, and humans,^{12–15} to our knowledge, very few studies have directly investigated the volume reduction of human pancreatic parenchyma as a risk factor for diabetes, and no previous study systematically quantified resection volumes in a population of patients. To study potential risk factors for new-onset diabetes in preoperatively non-diabetic patients, we sought to reliably quantify the volume reduction of human pancreatic parenchyma and to determine its longitudinal metabolic consequences following DP using multi-detector row computed tomography (MDCT) imaging volumetry.

Methods

Patients

A series of 98 consecutive patients who underwent DP at our institution between January 2005 and December 2011 was originally chosen from our prospectively maintained clinical database for this retrospective study. Data from 37 (38 %) of these candidates were excluded due to preoperative diabetes, as defined either by the WHO criteria of FPG ≥ 126 mg/dl detected on two or more separate days, or this abnormal FPG level detected once and plasma glucose ≥ 200 mg/dl measured 2 h after a 75-g glucose drink, or based on their treatment with oral anti-diabetic agents or insulin. The final study population consisted of 61 non-diabetic patients who had undergone DP.

Clinical data on pre- and postoperative patient status were obtained from existing medical records. Family histories of type 2 diabetes in first-degree relatives were also obtained. The preoperative data used for this study had been recorded within 14 days prior to surgery. Nutritional status and pancreatic endocrine functions were assessed based on measurements of body weight, serum albumin, FPG, and serum hemoglobin A1c (HbA1c). HbA1c values represent the National Glycohemoglobin Standardization Program (NGSP) equivalent values (in percent) and in all cases were converted from previous Japan Diabetes Society standard substance and measurement methods (JDS HbA1c, in percent) using the following formula: NGSP HbA1c (%) = JDS HbA1c (%) + 0.4 %. The percent resected volume (PRV) of pancreatic parenchyma, excluding tumor volume, was determined from abdominal MDCT measurements. Patient data were collected until the time of diagnosis of new-

onset diabetes or tumor recurrence. All 61 patients were followed up for at least 3 months.

For evaluating postoperative course, we defined and graded postoperative pancreatic fistula (POPF) using the classification methods of the International Study Group of Pancreatic Fistula,¹⁶ with POPF grade B or C defined as clinically important pancreatic fistula. Postoperative complications were designated as level I to V based on the Clavien classification.¹⁷

Determination of PRV of the Pancreatic Parenchyma

PRVs were determined retrospectively, using preoperative MDCT images in all patients. Continuous 0.8-mm 64-row MDCT images were acquired following administration of intravenous contrast material prior to surgery. MDCT data were transferred to a computer workstation (Aquarius; Elk, Osaka, Japan) for measurement of pancreas volume. To delineate the actual pancreatic resection lines, we compared preoperative CT with postoperative CT.

Excluding tumors, cystic lesions, any dilation in the pancreatic duct and bile duct, and vessels, we outlined the borders of the pancreatic parenchyma and the resection lines on every CT slice, and we then computed the resected and remnant areas of pancreatic parenchyma for each slice (Fig. 1). The volume (in milliliters) of the pancreatic parenchyma per slice was calculated as the product of the pancreas area (in square millimeters) times the slice thickness (in millimeters). Resected and remnant volumes of the pancreatic parenchyma were computed as the sum of the slice volumes. PRV was determined using the following formula: $PRV(\%) = [\text{resected volume of normal pancreas} \div \text{total volume of normal pancreas}] \times 100$. PRV was calculated in 52 cases.

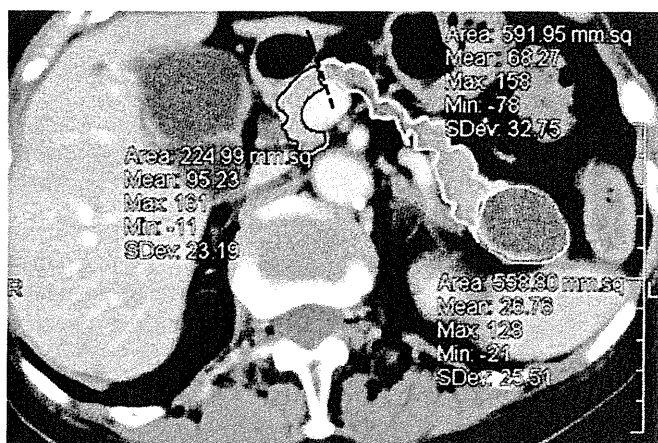


Fig. 1 MDCT pancreas volumetry. Outlined areas are the remnant parenchyma (black outline), resected parenchyma (light gray outline), and tumor (dark gray outline), excluding vessels. The dashed line is the pancreatic resection line. To determine percent resected volume, the volume (in milliliters) of the pancreatic parenchyma per slice was calculated as the product of the pancreas area (in square millimeters) times the slice thickness (in millimeters)

In the remaining nine cases, this value could not be measured accurately because of pancreatic edema or tumors with unclear borders that had invaded peri-pancreatic organs.

Definition of Postoperative New-Onset Diabetes

Postoperative new-onset diabetes was diagnosed retrospectively based on the WHO criteria of FPG ≥ 126 mg/dl detected on two or more separate days, or this abnormal FPG level detected once and plasma glucose ≥ 200 mg/dl measured in 2 h after a 75-g glucose drink. The onset day of diabetes was defined as the latter day on which abnormal blood test results were detected. In this study population, no patient was administered anti-diabetic therapy with oral agents or insulin before the development of diabetes, as defined by the criteria of this study.

Statistical Analysis

Patient characteristics are reported as means \pm standard deviation (SD), and results are presented as means \pm standard error (SE) or, where indicated, medians (range). Categorical variables are expressed numerically as percentages. For analyses of repeated measurements of body weight, serum albumin, FPG, and serum HbA1c prior to and 3, 6, and 12 months after surgery, we used an analysis of variance (ANOVA) and the Mauchly test, which evaluates the sphericity assumption. We used the Student's *t* test or Mann-Whitney test for continuous variables and Fisher's exact test for categorical variables. A multiple logistic regression analysis yielding odds ratios and 95 % confidence intervals (CIs) was used to identify risk factors for postoperative new-onset diabetes (with $p < 0.05$). The optimal HbA1c and PRV cutoffs for predicting the occurrence of postoperative new-onset diabetes were estimated using receiver operating characteristic (ROC) curves. All analyses were performed using JMP 9.0 for Macintosh (SAS Institute Inc, Cary, NC, USA).

Results

Patients' Characteristics

Physiological characteristics of the study patients are outlined in Table 1. While no patient met the WHO criteria for diabetes preoperatively, nine had impaired fasting glucose (IFG), defined as FPG of 110–125 mg/dl. The indications for DP included pancreatic tumors in 55 of the 61 patients (90 %, 25 malignant and 30 benign tumors), alcohol-induced chronic pancreatitis in three patients, autoimmune pancreatitis mimicking pancreatic cancer in two patients, and a pseudocyst following acute pancreatitis in one patient.

Table 1 Clinical characteristics of 61 non-diabetic patients who underwent distal pancreatectomy

Male patients	24 (39)
Age (years)	62 \pm 14
BMI (kg/m ²)	21.2 \pm 3.8
Preoperative HbA1c (%)	5.8 \pm 0.41
Preoperative IFG	9 (16)
Preoperative albumin (mg/dl)	4.0 \pm 0.64
Preoperative total cholesterol (mg/dl)	182 \pm 45
Preoperative pancreatic alpha-amylase (IU/l)	59 (4–264)
Operative time (min)	333 \pm 88
Intraoperative blood loss (ml)	427 (5–3524)
Malignancy	25 (41)
Percent resected volume (%)	38 \pm 17
POPF \geq grade B	16 (26)
Postoperative complication \geq Clavien's grade II	22 (36)
Postoperative hospital stay (days)	18 (7–58)
Mortality (%)	0

Values are means \pm SD, medians (range), or *n* (%)

HbA1c hemoglobin A1c, *IFG* impaired fasting glucose, *FPG* fasting plasma glucose, *POPF* postoperative pancreatic fistula

Three patients had a first-degree family history of type 2 diabetes.

Pancreas Volumetry

MDCT imaging volumetric data showed a wide range of volumes of whole, remnant, and resected pancreatic parenchyma and of tumors in patients with or without new-onset diabetes (Table 2). While the mean PRV for all 61 cases was 38 % (range 9–85 %), the mean PRV for the new-onset diabetes group was 49 %, which was significantly higher than the PRV of 32 % for the non-diabetic group.

Sequential Changes in Diabetic and Nutritional Status After Surgery

We compared four physiological parameters in new-onset diabetic versus non-diabetic patients at four time points: before and 3, 6, and 12 months after surgery. Three months after surgery, there were significant increases in FPG and HbA1c in both groups (Table 3). Disturbances in glucose control occurred within the first 3 months after surgery, and did not significantly progress after that time in either group.

During the post-DP follow-up period (median 26 months, range 3–88 months), 22 patients (36 %) developed new-onset diabetes (median onset time 8 months, range 0.5–42 months). In most of the 39 patients without new-onset diabetes, FPG and HbA1c increased significantly during the follow-up period; however, values remained stable in eight

Table 2 CT volumetry in DP patients

	All patients	New-onset diabetes group	No new-onset diabetes group	<i>p</i> value
Number of patients with PRV data	52	20	32	
Whole normal parenchyma (ml)	56.6 (16.0–128.2)	54.6 (27.0–89.4)	56.6 (16.0–128.2)	0.58
Remnant normal parenchyma (ml)	36.5 (4.4–116.4)	25.1 (4.4–65.8)	38.6 (6.6–116.4)	0.047
Resected normal parenchyma (ml)	18.7 (3.5–57.7)	25.8 (9.9–57.7)	16.5 (3.5–55.3)	0.004
Tumor or cystic lesion (ml)	5.4 (0–543.7)	4.1 (0–38.7)	7.4 (0.2–543.7)	0.11
PRV (%)	38±17 (9–85)	49±15 (20–85)	32±15 (9–59)	< 0.001

Values are medians (range) or means±SD (range). *p* values were obtained using Mann–Whitney *U* test, except for use of Student's *t* test for PRV CT computed tomography, DP distal pancreatectomy

of these 39 patients (change in HbA1c≤0.1 %), and one patient displayed improvement in glycemic control, as exhibited by a 0.4 % decrease in HbA1c.

While we observed significant between-group differences in the changes in FPG (Fig. 2a) (*p*=0.003) and HbA1c (Fig. 2b) (*p*<0.001) over time, there were no significant differences in changes in body weight (Fig. 2c) (*p*=0.36) or serum albumin (Fig. 2d) (*p*=0.58). Because Mauchly tests for the sphericity assumption were not significant for these factors (*P*=0.21, 0.82, 0.28, and 0.30, respectively), the reported *p* values are for univariate ANOVA.

Risk Factors for Postoperative New-Onset Diabetes

Univariate analyses identified three statistically significant risk factors for postoperative new-onset diabetes: preoperative HbA1c≥5.7 %, PRV>44 %, and age (Table 4). Multivariate logistic regression analysis also identified HbA1c≥5.7 % [odds ratio 15.6 (95 % CI 2.80–147), *p*=0.001] and PRV>44 % [odds ratio 11.3 (95% CI 2.12–92.1), *p*=0.004] as independent risk factors for postoperative new-onset

diabetes (Table 5). Regarding family history, one of three patients with first-degree family history of type 2 diabetes, of whom PRV was 85 %, developed new-onset diabetes at 2 months after surgery. We assessed the sensitivity and specificity of the HbA1c and PRV parameters using the ROC curves. The areas under the ROC curves were 0.831 for HbA1c and 0.793 for PRV. Using these curves, HbA1c of 5.7 % and PRV of 44 % were determined to be the cutoffs for predicting the occurrence of postoperative diabetes. The sensitivity, specificity, and positive and negative predictive values derived from these curves were 0.82, 0.64, 0.56, and 0.86 for HbA1c and 0.75, 0.81, 0.71, and 0.84 for PRV, respectively.

Discussion

We report here two major findings from this study of patients who underwent DP. First, in the majority of preoperatively non-diabetic patients, DP led to disturbances in glucose metabolism, and there was a 36 % incidence of

Table 3 FPG and serum HbA1c before and 3, 6, and 12 months after surgery

	All patients (<i>n</i> =61)	<i>p</i> value	New-onset diabetes group (<i>n</i> =22)	<i>p</i> value	No new-onset diabetes group (<i>n</i> =39)	<i>p</i> value
FPG (mg/dl)						
Before surgery	96±1.9		101±3.8		93±1.9	
3 months after surgery	109±2.8	<0.001 ^a	121±5.3	0.008 ^a	102±2.6	0.006 ^a
6 months after surgery	111±4.9	0.29 ^b	133±11.6	0.17 ^b	99±2.4	0.75 ^b
12 months after surgery	114±5.8	0.19 ^b	137±12.2	0.15 ^b	100±3.0	0.55 ^b
HbA1c (%)						
Before surgery	5.8±0.05		6.1±0.06		5.6±0.06	
3 months after surgery	6.2±0.10	<0.001 ^a	6.7±0.19	0.003 ^a	5.9±0.07	0.002 ^a
6 months after surgery	6.3±0.24	0.73 ^b	7.0±0.51	0.81 ^b	5.9±0.07	1.00 ^b
12 months after surgery	6.4±0.18	0.13 ^b	7.1±0.36	0.49 ^b	5.9±0.06	0.059 ^b

Values are means±SE. Data were analyzed using Student's paired *t* test for each group

^aDifferences compared to values before surgery

^bDifferences compared to values at 3 months after surgery

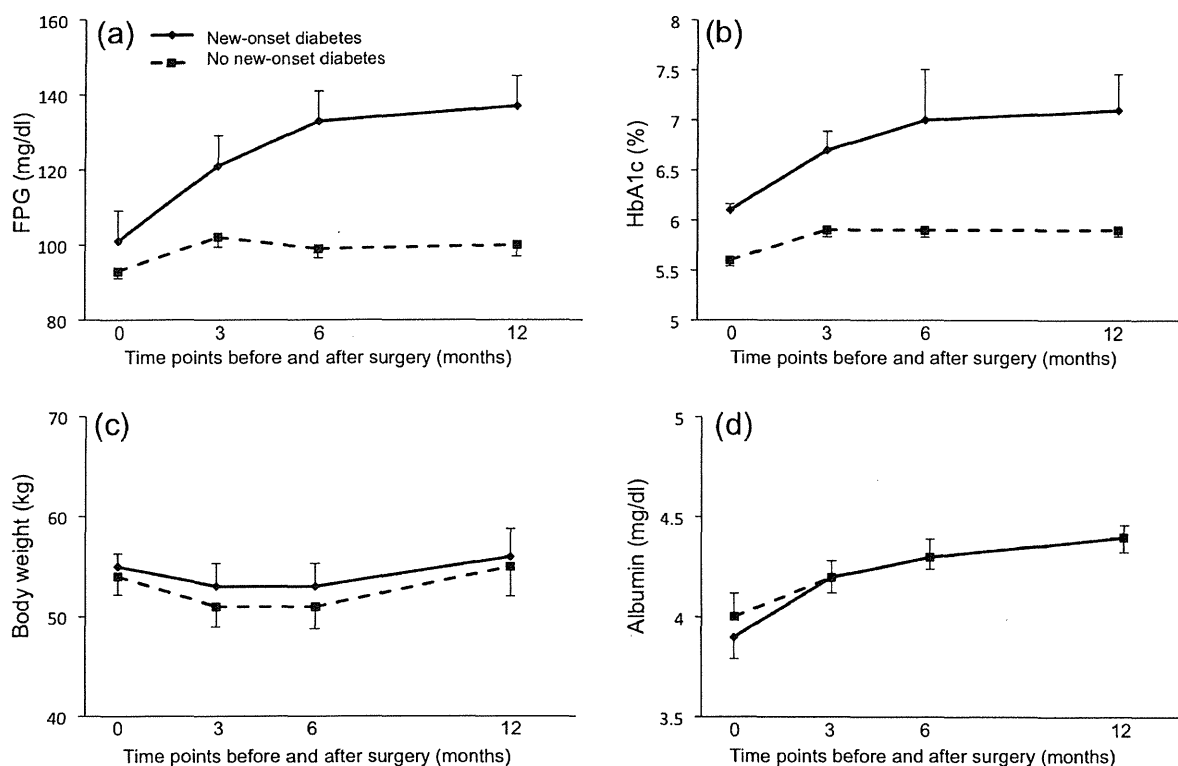


Fig. 2 Changes in parameters before and 3, 6, and 12 months after surgery: **a** FPG, **b** HbA1c, **c** body weight, and **d** serum albumin. Values from patients who developed new-onset diabetes (*solid lines*) were compared with non-diabetic patients (*dashed lines*) using ANOVA, with evaluation of the sphericity assumption by the Mauchly test.

Postoperatively, there were significant between-group differences in changes in FPG ($p=0.003$) and HbA1c levels ($p<0.001$). No significant between-group difference in body weight ($p=0.36$) or albumin ($p=0.58$) was observed.

new-onset diabetes postoperatively. Second, in DP patients, PRV and preoperative HbA1c were independent risk factors for new-onset diabetes.

Our results enable us to provide evidence-based preoperative counseling and individualized postoperative surveillance. Prior to surgery, we can now offer patients specific information about their individual risk of postoperative diabetes. Postoperatively, appropriate surveillance may detect the development of impaired glucose metabolism [i.e., impaired glucose tolerance (IGT), IFG, and diabetes] at an early stage and enable early intervention. Intensive glucose control has been reported to decrease the risks of major cardiovascular events and death in patients with newly diagnosed type 2 diabetes.¹⁸ Also, in patients with IGT who are pre-diabetic, the early introduction of anti-diabetic agents has been reported to diminish the development of type 2 diabetes.¹⁹ The American Diabetes Association recommends intensive annual monitoring, lifestyle modification, and sometimes use of anti-diabetic agents in patients with IGT, IFG, or HbA1c of 5.7–6.4 % for the prevention and delay of developing type 2 diabetes.²⁰ Therefore, early detection and intervention for endocrine insufficiency are essential for DP patients.

Prior reports have estimated the incidence of new-onset diabetes after DP at between 9 and 38 % of preoperatively

non-diabetic patients.^{4,6,8,21} The numerous limitations of these studies (such as unspecified preoperative diabetic status of study patients, inconsistent standards for diagnosis of postoperative diabetes, and selection of cohorts of patients with chronic pancreatitis) make it difficult to evaluate the basis for this wide range of diabetes incidence. In the current study, the incidence of postoperative new-onset diabetes in preoperatively non-diabetic patients was 36 %. We attribute this relatively high measure of incidence to our application of a definitive classification system and close follow-up.

The results of this study identify PRV >44 % as an independent risk factor for postoperative new-onset diabetes in preoperatively non-diabetic DP patients. Although beta cell mass has previously been reported to be significantly related to plasma glucose control,^{14,22,23} volumetric assessments in relation to postoperative endocrine function of the pancreas remain scarce. Previous studies in large animals^{13,15} and humans²² have demonstrated that a 50 % loss in beta cells elevates plasma glucose. The DP procedure is often referred to as a “hemi-pancreatectomy,” with an estimated 50 % reduction in pancreatic volume after transection on the superior mesenteric vein (SMV).^{9,11} In our study, the median PRV in 29 patients with transection on the SMV was 46 %, but we observed a wide range of values in these cases (PRV from 18 to 67 %), as well as among all

Table 4 Univariate analysis of risk factors for postoperative new-onset diabetes

	New-onset diabetes group (<i>n</i> =22)	No new-onset diabetes group (<i>n</i> =39)	<i>p</i> value
Male patients	9 (41)	15 (38)	1.00 ^a
Age (years)	67±3.0	59±2.2	0.025 ^b
BMI (kg/m ²)	22±0.78	20±0.59	0.075 ^b
Preoperative HbA1c≥5.7 %	18 (82)	14 (36)	0.001 ^a
Preoperative IFG	6 (27)	3 (8)	0.059 ^a
Preoperative albumin (mg/dl)	3.9±0.13	4.0±0.10	0.59 ^b
Preoperative total cholesterol (mg/dl)	176±9.6	186±7.3	0.42 ^b
Preoperative pancreatic alpha-amylase (IU/l)	58 (6–243)	59 (4–264)	0.98 ^c
Operative time (min)	312±19	347±15	0.14 ^b
Intraoperative blood loss (ml)	372 (5–1125)	527 (5–3524)	0.17 ^c
Malignancy	8 (36)	17 (44)	0.79 ^a
PRV>44 %	15 (75)	6 (19)	<0.001 ^a
POPF ≥ grade B	6 (27)	10 (26)	1.00 ^a
Postoperative complication ≥ Clavien's grade II	7 (32)	15 (38)	0.78 ^a
Postoperative hospital stay (days)	16 (7–54)	18 (7–58)	0.60 ^c
Adjuvant chemotherapy	7 (32)	15 (38)	0.78 ^a

Values are means±SE, medians (range) or *n* (%)

HbA1c hemoglobin A1c, FPG fasting plasma glucose, POPF postoperative pancreatic fistula

^a*p* values were obtained using Fisher's exact test

^b*p* values were obtained using Student's *t* test

^c*p* values were obtained using Mann–Whitney *U* test

cases of DP (PRV from 9 to 85 %). Variations in PRV can also be attributed to differences in the patients' pancreatic sizes and shapes, as well as differences in pancreatic tumor characteristics (i.e., location and the involvement of the main pancreatic duct that causes atrophy of the distal pancreas). Our use of MDCT-based measurements of pancreas volume resulted in more precise PRV values and thereby provides evidence that greater resection of pancreatic tissue increases the incidence of new-onset diabetes in preoperatively non-diabetic DP patients. Thus, although pancreatic resection must be tailored to suit the tumor character (benign or malignant), location, and extent of tumor invasion, our data suggest that parenchyma-sparing pancreatectomies (such as middle pancreatectomy or tumor enucleation) are more likely to maintain postoperative pancreatic endocrine function and reduce the risk of diabetes.

In this study, we frequently observed a delay in diabetes onset in the 22 new-onset diabetics (median time 8 months, range 0.5–42 months), with only five showing signs of

diabetes within 3 months. However, both groups of DP patients displayed significant increases in FPG and HbA1c levels within 3 months following surgery, but without further increases thereafter. These data lead us to hypothesize that, while surgical reduction of pancreatic parenchyma volume quickly impairs glucose metabolism, the observed lag in diabetes onset depends on other factors, such as the amount and overall health of the remaining endocrine pancreas that control plasma glucose.

In patients with insufficient functional reserve of the remnant pancreas to compensate for beta cell deficit (with severity depending on the volume of the pancreas removed), overt diabetes would develop in the early postoperative period (within 3 months postoperatively). The functional reserve of the endocrine pancreas could be estimated based on the preoperative HbA1c value, which was identified as a risk factor predictive of postoperative diabetes in this study. In patients with late-onset diabetes (later than 3 months after surgery), beta cell compensation would considerably influence the diabetes onset time. In the field of islet cell transplants, although obese individuals are generally at high risk of diabetes, it has been reported that the high demand for insulin in obese donors without diabetes promotes the necessary increase in islet cell hypertrophy and proliferation.²⁴ Islet cells that remain after pancreatectomy are likely in a similar situation that stimulates islet hypertrophy and thus a compensatory increase in insulin secretion in the endocrine pancreas. Eventually, however, this pre-diabetic state may progress to overt diabetes once the endocrine pancreas is exhausted and fails to control glucose homeostasis. Also,

Table 5 Multivariate logistic regression analysis of risk factors for postoperative new-onset diabetes

	Odds ratio	95 % CI	<i>p</i> value
Age	1.03 ^a	0.96–1.11	0.42
Preoperative IFG	1.52	0.18–14.7	0.69
Preoperative HbA1c≥5.7 %	15.6	2.80–147	0.001
PRV>44 %	11.3	2.12–92.1	0.004

^aOdds ratio by 1 year post-DP

additional factors that vary the timing of late-onset postoperative diabetes include normal progression of underlying diseases, such as pancreatitis, as well as acquired risk factors for type 2 diabetes (e.g., weight gain or aging).

Our analyses identified preoperative HbA1c as a second risk factor for postoperative new-onset diabetes. HbA1c is increasingly viewed as a superior index of chronic hyperglycemia relative to plasma glucose (which varies during the day), and the American Diabetes Association recently added HbA1c ≥ 6.5 % to its diagnostic criteria for the detection of early diabetes, with slightly lower HbA1c values (from 5.7 to 6.4 %) categorized as signaling an increased risk of diabetes.¹ In our study, the cutoff value at which HbA1c became a risk factor was 5.7 %. Among the study's 61 patients (none of whom met the WHO criteria for diabetes, FPG ≥ 126 mg/dl), preoperative HbA1c was ≥ 6.5 % in two patients and between 5.7 and 6.4 % in another 30 patients. Of these 32 individuals, 18 patients (56 %) developed postoperative diabetes. However, it is noteworthy that four additional patients with HbA1c < 5.7 %, but relatively high PRV (from 47 to 61 %), also developed diabetes.

The metabolic consequences of pancreatic resection are multifaceted and can be affected by glucoregulatory hormone concentrations, the balance between production and utilization of glucose, changes in insulin sensitivity and nutritional status, surgical complications,^{25,26} and tumor character (malignant or benign). Despite decreases in insulin secretion, some studies have reported post-pancreatectomy improvements in glucose control in malignant cases.^{27,28} Because malignant pancreatic tumors are known to produce substances that impair the action of insulin and decrease insulin sensitivity, a patient's diabetic status can sometimes improve after tumor removal.^{29,30} Of the nine patients in our study who showed stable glycemic control (eight with HbA1c ≤ 0.1 %) or improved control (one with HbA1c reduced by 0.4 %) during the post-DP follow-up period, five had malignant tumors. The one patient with improved glycemic control had a highly advanced cancer, as well as preoperative HbA1c and BMI levels of 6.2 % and 28.7 kg/mm², respectively, indicating pre-diabetes. This patient lost 13 % of his body weight within 3 months after surgery, and it is likely that this loss helped suppress the progression of type 2 diabetes. Our results did not demonstrate any influence of malignant tumors on postoperative endocrine function.

Conclusion

Adequate preoperative functional reserve of the endocrine pancreas (HbA1c < 5.7 %) and maximizing the volume of the pancreatic parenchyma preserved are two key determinants of successful postoperative glycemic control. Our

findings enable reliable preoperative evaluation of the risk of developing diabetes and to perform postoperative surveillance appropriately. Late-onset diabetes needs to be recognized as a common sequela of DP, and longitudinal follow-up and preventive intervention (weight control and anti-diabetic agents for pre-diabetic patients) should be introduced in high-risk patients.

Open Access This article is distributed under the terms of the Creative Commons Attribution License which permits any use, distribution, and reproduction in any medium, provided the original author(s) and the source are credited.

References

1. Diagnosis and classification of diabetes mellitus. *Diabetes Care* 2012; 35 Suppl 1: S64–71.
2. Ewald N, Kaufmann C, Raspe A, Kloer HU, Bretzel RG, Hardt PD. Prevalence of diabetes mellitus secondary to pancreatic diseases (type 3c). *Diabetes Metab Res Rev* 2011; 28: 338–42.
3. Hardt PD, Brendel MD, Kloer HU, Bretzel RG. Is pancreatic diabetes (type 3c diabetes) underdiagnosed and misdiagnosed? *Diabetes Care* 2008; 31 Suppl 2: S165–169.
4. King J, Kazanjian K, Matsumoto J, Reber HA, Yeh MW, Hines OJ, Eibl G. Distal pancreatectomy: incidence of postoperative diabetes. *J Gastrointest Surg* 2008; 12: 1548–1553.
5. Crippa S, Bassi C, Warshaw AL, Falconi M, Partelli S, Thayer SP, Pederzoli P, Fernandez-del Castillo C. Middle pancreatectomy: indications, short- and long-term operative outcomes. *Ann Surg* 2007; 246: 69–76.
6. Shikano T, Nakao A, Kodera Y, Yamada S, Fujii T, Sugimoto H, Kanazumi N, Nomoto S, Takeda S. Middle pancreatectomy: safety and long-term results. *Surgery* 2010; 147: 21–29.
7. DiNorcia J, Ahmed L, Lee MK, Reavey PL, Yakaitis EA, Lee JA, Schroppe BA, Chabot JA, Allendorf JD. Better preservation of endocrine function after central versus distal pancreatectomy for mid-gland lesions. *Surgery* 2010; 148: 1247–1254; discussion 1254–1246.
8. Riediger H, Adam U, Fischer E, Keck T, Pfeffer F, Hopt UT, Makowiec F. Long-term outcome after resection for chronic pancreatitis in 224 patients. *J Gastrointest Surg* 2007; 11: 949–959.
9. Menge BA, Schrader H, Breuer TG, Dabrowski Y, Uhl W, Schmidt WE, Meier JJ. Metabolic consequences of a 50% partial pancreatectomy in humans. *Diabetologia* 2009; 52: 306–317.
10. Kumar AF, Gruessner RW, Seaquist ER. Risk of glucose intolerance and diabetes in hemipancreatectomized donors selected for normal preoperative glucose metabolism. *Diabetes Care* 2008; 31: 1639–1643.
11. Robertson RP, Lanz KJ, Sutherland DE, Seaquist ER. Relationship between diabetes and obesity 9 to 18 years after hemipancreatectomy and transplantation in donors and recipients. *Transplantation* 2002; 73: 736–741.
12. Leahy JL, Bonner-Weir S, Weir GC. Abnormal glucose regulation of insulin secretion in models of reduced B-cell mass. *Diabetes* 1984; 33: 667–673.
13. Matveyenko AV, Veldhuis JD, Butler PC. Mechanisms of impaired fasting glucose and glucose intolerance induced by an approximate 50% pancreatectomy. *Diabetes* 2006; 55: 2347–2356.
14. Meier JJ, Menge BA, Breuer TG, Muller CA, Tannapfel A, Uhl W, Schmidt WE, Schrader H. Functional assessment of pancreatic beta-cell area in humans. *Diabetes* 2009; 58: 1595–1603.

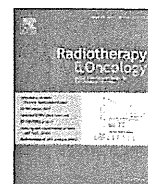
15. Saisho Y, Butler AE, Manesso E, Galasso R, Zhang L, Gurlo T, Toffolo GM, Cobelli C, Kavanagh K, Wagner JD, Butler PC. Relationship between fractional pancreatic beta cell area and fasting plasma glucose concentration in monkeys. *Diabetologia* 2010; 53: 111–114.
16. Bassi C, Dervenis C, Butturini G, Fingerhut A, Yeo C, Izbicki J, Neoptolemos J, Sarr M, Traverso W, Buchler M. Postoperative pancreatic fistula: an international study group (ISGPF) definition. *Surgery* 2005; 138: 8–13.
17. Dindo D, Demartines N, Clavien P-A. Classification of Surgical Complications. *Ann Surg* 2004; 240: 205–213.
18. Holman RR, Paul SK, Bethel MA, Matthews DR, Neil HA. 10-year follow-up of intensive glucose control in type 2 diabetes. *N Engl J Med* 2008; 359: 1577–1589.
19. Kawamori R, Tajima N, Iwamoto Y, Kashiwagi A, Shimamoto K, Kaku K. Voglibose for prevention of type 2 diabetes mellitus: a randomised, double-blind trial in Japanese individuals with impaired glucose tolerance. *Lancet* 2009; 373: 1607–1614.
20. Standards of medical care in diabetes—2012. *Diabetes Care* 2012; 35 Suppl 1: S11–63.
21. Hutchins RR, Hart RS, Pacifico M, Bradley NJ, Williamson RC. Long-term results of distal pancreatectomy for chronic pancreatitis in 90 patients. *Ann Surg* 2002; 236: 612–618.
22. Ritzel RA, Butler AE, Rizza RA, Veldhuis JD, Butler PC. Relationship between beta-cell mass and fasting blood glucose concentration in humans. *Diabetes Care* 2006; 29: 717–718.
23. Nakamura Y, Higuchi S, Maruyama K. Pancreatic volume associated with endocrine and exocrine function of the pancreas among Japanese alcoholics. *Pancreatology* 2005; 5: 422–431.
24. Matsumoto I, Sawada T, Nakano M, Sakai T, Liu B, Ansite JD, Zhang HJ, Kandaswamy R, Sutherland DE, Hering BJ. Improvement in islet yield from obese donors for human islet transplants. *Transplantation* 2004; 78: 880–885.
25. Ishikawa O, Ohigashi H, Eguchi H, Yokoyama S, Yamada T, Takachi K, Miyashiro I, Murata K, Doki Y, Sasaki Y, Imaoka S. Long-term follow-up of glucose tolerance function after pancreaticoduodenectomy: comparison between pancreaticogastrostomy and pancreaticojejunostomy. *Surgery* 2004; 136: 617–623.
26. Murakami Y, Uemura K, Hayashidani Y, Sudo T, Hashimoto Y, Ohge H, Sueda T. Long-term pancreatic endocrine function following pancreatoduodenectomy with pancreaticogastrostomy. *J Surg Oncol* 2008; 97: 519–522.
27. Litwin J, Dobrowolski S, Orłowska-Kunikowska E, Sledzinski Z. Changes in glucose metabolism after Kausch–Whipple pancreatectomy in pancreatic cancer and chronic pancreatitis patients. *Pancreas* 2008; 36: 26–30.
28. Permert J, Ihse I, Jorfeldt L, von Schenck H, Arnquist HJ, Larsson J. Improved glucose metabolism after subtotal pancreatectomy for pancreatic cancer. *Br J Surg* 1993; 80: 1047–1050.
29. Katsumichi I, Pour PM. Diabetes mellitus in pancreatic cancer: is it a causal relationship? *Am J Surg* 2007; 194: S71–75.
30. Saruc M, Pour PM. Diabetes and its relationship to pancreatic carcinoma. *Pancreas* 2003; 26: 381–387.



Contents lists available at SciVerse ScienceDirect

Radiotherapy and Oncology

journal homepage: www.thegreenjournal.com



Proton RT in pancreatic cancer

A phase I/II study of gemcitabine-concurrent proton radiotherapy for locally advanced pancreatic cancer without distant metastasis[☆]

Kazuki Terashima^{a,*}, Yusuke Demizu^a, Naoki Hashimoto^a, Dongcun Jin^a, Masayuki Mima^a, Osamu Fujii^a, Yasue Niwa^a, Kento Takatori^b, Naoto Kitajima^b, Sachiyo Sirakawa^c, Ku Yonson^c, Yoshio Hishikawa^a, Mitsuyuki Abe^a, Ryohei Sasaki^d, Kazuro Sugimura^e, Masao Murakami^a

^a Department of Radiology, Hyogo Ion Beam Medical Center; ^b Department of Internal Medicine, Kasai City Hospital; ^c Division of Hepato-Biliary-Pancreatic Surgery, Kobe University Graduate School of Medicine; ^d Division of Radiation Oncology, Kobe University Graduate School of Medicine; ^e Division of Radiology, Kobe University Graduate School of Medicine, Hyogo, Japan

ARTICLE INFO

Article history:

Received 20 August 2011

Received in revised form 15 December 2011

Accepted 20 December 2011

Available online 31 January 2012

Keywords:

Proton radiotherapy

Gemcitabine

Pancreatic cancer

Locally advanced

Chemoradiotherapy

ABSTRACT

Purpose: We conducted the study to assess the feasibility and efficacy of gemcitabine-concurrent proton radiotherapy (GPT) for locally advanced pancreatic cancer (LAPC).

Materials and methods: Of all 50 patients who participated in the study, 5 patients with gastrointestinal (GI)-adjacent LAPC were enrolled in P-1 (50 Gy equivalent [GyE] in 25 fractions) and 5 patients with non-GI-adjacent LAPC in P-2 (70.2 GyE in 26 fractions), and 40 patients with LAPC regardless of GI-adjacency in P-3 (67.5 GyE in 25 fractions using the field-within-a-field technique). In every protocol, gemcitabine (800 mg/m²/week for 3 weeks) was administered concurrently. Every patient received adjuvant chemotherapy including gemcitabine after GPT within the tolerable limit.

Results: The median follow-up period was 12.5 months. The scheduled GPT was feasible for all except 6 patients (12%) due to acute hematologic or GI toxicities. Grade 3 or greater late gastric ulcer and hemorrhage were seen in 5 patients (10%) in P-2 and P-3. The one-year freedom from local-progression, progression-free, and overall survival rates were 81.7%, 64.3%, and 76.8%, respectively.

Conclusion: GPT was feasible and showed high efficacy. Although the number of patients and the follow-up periods are insufficient, the clinical results seem very encouraging.

© 2012 Elsevier Ireland Ltd. All rights reserved. Radiotherapy and Oncology 103 (2012) 25–31

The prognosis of pancreatic cancer is poor, with a five-year survival rate of about 5% in total [2]. Only radical surgical resection has been shown to cure the condition, although the five-year survival rate remains low at about 10–20%. And only 15–20% of all patients with pancreatic cancer can be treated by resection, while the other patients cannot undergo resection because of local invasion or distant metastasis at diagnosis [4,9].

For the treatment of non-resectable pancreatic cancers, chemoradiotherapy (CRT) with concurrent 5-fluorouracil (5-FU) is historically considered the standard therapy for locally advanced pancreatic cancer (LAPC) [6,18,26]. Recently, based on a background of favorable results of gemcitabine-based chemotherapy [1,9], and the fact that gemcitabine is a potent radio-sensitizer [16], many studies on gemcitabine-concurrent CRT have been performed for LAPC [7,17,20,24], and indicate the possibility of an improvement in survival. These studies have shown that reduction

of the irradiation doses and target fields was necessary when gemcitabine was administered at or near the full dose (1000 mg/m²). In contrast, a reduction of the gemcitabine dose was needed when irradiation was administered at doses over 50 Gy, which is necessary for the local control of malignant tumors. The reason for these restrictions of the chemoradiotherapy was speculation that the region of gastrointestinal (GI) tract located near the pancreas was irradiated beyond tolerable doses. Consequently, we thought that proton beam radiotherapy could deliver higher dose above 50 Gy concurrently with a higher dose of gemcitabine to a larger field containing the draining and paraaortic lymph nodes and peripheral regions surrounding the celiac artery and superior mesenteric artery.

Radiotherapy using protons or carbon-ions is currently attracting worldwide interest because of its physical properties including superior dose distribution to a target, which allows selective irradiation to the tumor, while minimizing irradiation of the surrounding normal tissues [10,15,25]. In our pilot study, proton beam radiotherapy alone was performed at doses of 40 and 50 GyE for patients with LAPC between November 2004 and October 2006 [12]. Although local control and survival did not reach significance in

[☆] This study has not been presented previously.

* Corresponding author. Address: Department of Radiology, Hyogo Ion Beam Medical Center, 1-2-1 Kouto, Shingu-cho, Tatsuno, Hyogo 679-5165, Japan.

E-mail address: terashima@kmyr.jp (K. Terashima).

comparison with other treatments, such as chemotherapy alone or CRT, we confirmed the feasibility and safety of proton radiotherapy. Based on this pilot study, we started gemcitabine-concurrent proton radiotherapy (GPT) for LAPC to assess the feasibility and efficacy of this regimen. To our knowledge, this is the first report on the clinical use of concurrent gemcitabine and proton radiotherapy for the treatment of pancreatic cancer.

Patients and methods

Patient eligibility

Patients with LAPC which was defined as borderline resectable cancer and unresectable cancer without distant metastases [28], that was cytologically or histologically confirmed to be adenocarcinoma, with an Eastern Cooperative Oncology Group (ECOG) performance status of 0–2, and were in adequate physical condition to tolerate chemotherapy were eligible for this study. Patients with a history of abdominal radiotherapy or previous treatment of pancreatic tumor were excluded.

All patients provided written informed consent prior to enrollment. The study was approved by the institutional review board and registered on the University Hospital Medical Information Network Clinical Trials Registry (UMIN-CTR, <http://www.umin.ac.jp/ctr>, UMIN ID: UMIN00002173).

Pretreatment workup

At baseline, all patients underwent an abdominal contrast-enhanced computed tomography (CT) scan, chest CT scan, positron emission tomography with ^{18}F -fluorodeoxy glucose (FDG-PET), and gastrointestinal fiberoptic (GIF) and were assessed for tumor markers (CA19-9, CEA, DUPAN-2, and SPAN-1). The disease was staged according to the International Union Against Cancer (UICC) TNM staging system, 6th edition.

Treatment regimen

Concurrent and adjuvant chemotherapy

In all protocols, all patients were scheduled to receive intra-venous infusion of gemcitabine (800 mg/m^2) for 30 min for the initial 3 weeks (days 1, 8, and 15) during 5 weeks of proton radiotherapy. We determined the dose of gemcitabine according to the studies by Casper et al. [3] and Burris et al. [1], and the schedule according to the study by Murphy et al. [20]. Gemcitabine was administered if the absolute granulocyte count was $>2000/\text{mm}^3$ and the platelet count was $>70000/\text{m}^3$ on the scheduled day.

Following GPT, all patients received systemic gemcitabine-based chemotherapy for as long as possible.

Proton radiotherapy

Hyogo Ion Beam Medical Center (HIBMC) treats patients with both proton and carbon-ion beams. We decided to use proton therapy for this study, because proton beams can be delivered to the target from any direction by using a rotating gantry so that irradiation of the GI tract is minimized. However, a rotating gantry is not available for carbon ion therapy. Furthermore, we anticipated that the administration of gemcitabine would have a sensitizing effect on proton therapy, as previously shown in human pancreatic cancer cells [5].

The patients were treated with 150–210 MeV proton beams. A respiratory gating system was used for all patients to irradiate the beam during the exhalation phase. Patient set-up was performed daily by subtraction of the 2 sets of orthogonal digital radiographs before irradiation. The translation and rotation of the

patient detected by the positioning system were compensated for by adjustment of the treatment couch. The setup was continued until the bony landmarks on the digitally reconstructed radiographs agreed within 1 mm. The biologic effects of proton therapy at our institution were evaluated *in vitro* and *in vivo*. The relative biologic effectiveness (RBE) values were determined to be 1.1 by biologic experiments [11]. Because all tissues are assumed to have almost the same RBE, doses expressed in GyE are directly comparable to photon doses.

Treatment planning

Proton beam treatment plans were developed using a CT-based 3-dimensional treatment planning system. The gross tumor volume (GTV) was defined as the primary tumor plus the apparent lymph nodes as determined by a fusion contrast-enhanced CT subsidiary using FDG-PET. The clinical target volume (CTV) comprised the addition of a 5-mm margin to the GTV and prophylactic irradiation regions containing the draining lymph nodes and paraaortic lymph nodes as well as peripheral regions surrounding the celiac artery and superior mesenteric artery. We defined the CTV to contain the prophylactic region because metastases to regional lymph nodes have been recognized as prognostic factors in some studies of CRT [8] and resection [23,27] for LAPC. The planning target volume (PTV) was defined as the CTV plus a setup margin (5 mm) and a respiratory gating margin (1–5 mm), which was measured on CT images between inspiratory and expiratory phases. In general, the stomach, small bowel including the duodenum, kidneys, and spinal cord were defined as organs-at-risk (OAR). The dose restrictions for stomach, duodenum, and spinal cord were approximately 50 GyE, 50 GyE, and 45 GyE, respectively [13,14]. Additionally, we planned the irradiated volumes of the stomach, duodenum, and kidneys to be as small as possible.

Dose-fractionation

A total of 3 protocols were used in this study. In the early phase of the study, 2 protocols were used contemporaneously; protocol P-1 (50 GyE in 25 fractions) was used for patients with GI-adjacent LAPC, and P-2 (70.2 GyE in 26 fractions) was used for those with non-GI-adjacent LAPC. The non-GI-adjacent LAPC were defined as tumors that could be treated with irradiation plans that covered the GTV: over 95% of the prescribed dose in P-2 (70.2 GyE), which kept the dose administered to the GI-tract under 50 GyE. The others were defined as GI-adjacent LAPC who were treated with P-1. After the early phase, all patients were treated with protocol P-3 (67.5 GyE in 25 fractions) using the field-within-a-field technique.

In P-1, a total dose of 50 GyE was delivered in 25 fractions over 5 weeks to the PTV, based on our pilot study [12] and the report of 5-FU-concurrent CRT [19], in which irradiation doses of 39.6–50.4 Gy did not result in any late GI toxicity. In P-2, 70.2 GyE in 26 fractions over 6 weeks was delivered to the PTV. This approach was designed based on our experiences in treating head and neck cancers and lung cancer as well as other tumors, in which 70.2 GyE in 26 fractions was employed after dose escalation from 65 GyE in 26 fractions [21].

In P-3, 67.5 GyE in 25 fractions over 5 weeks was delivered using the field-within-a-field technique. With this technique, we used three types of split doses: $2 + 0.7\text{ GyE}$, $1.8 + 0.9\text{ GyE}$, and $1.6 + 1.1\text{ GyE}$. For example, we delivered 1.8 GyE to the whole PTV (Fig. 1a) and 0.9 GyE to the PTV excluding the GI tract including stomach, small bowel, and large bowel, in one fraction (Fig. 1b). Consequently, a maximum dose of 2.7 GyE was administered as a single fraction (total 67.5 GyE) to the majority of the PTV (Fig. 1c), in parallel with limiting the dose to the GI tract to approximately

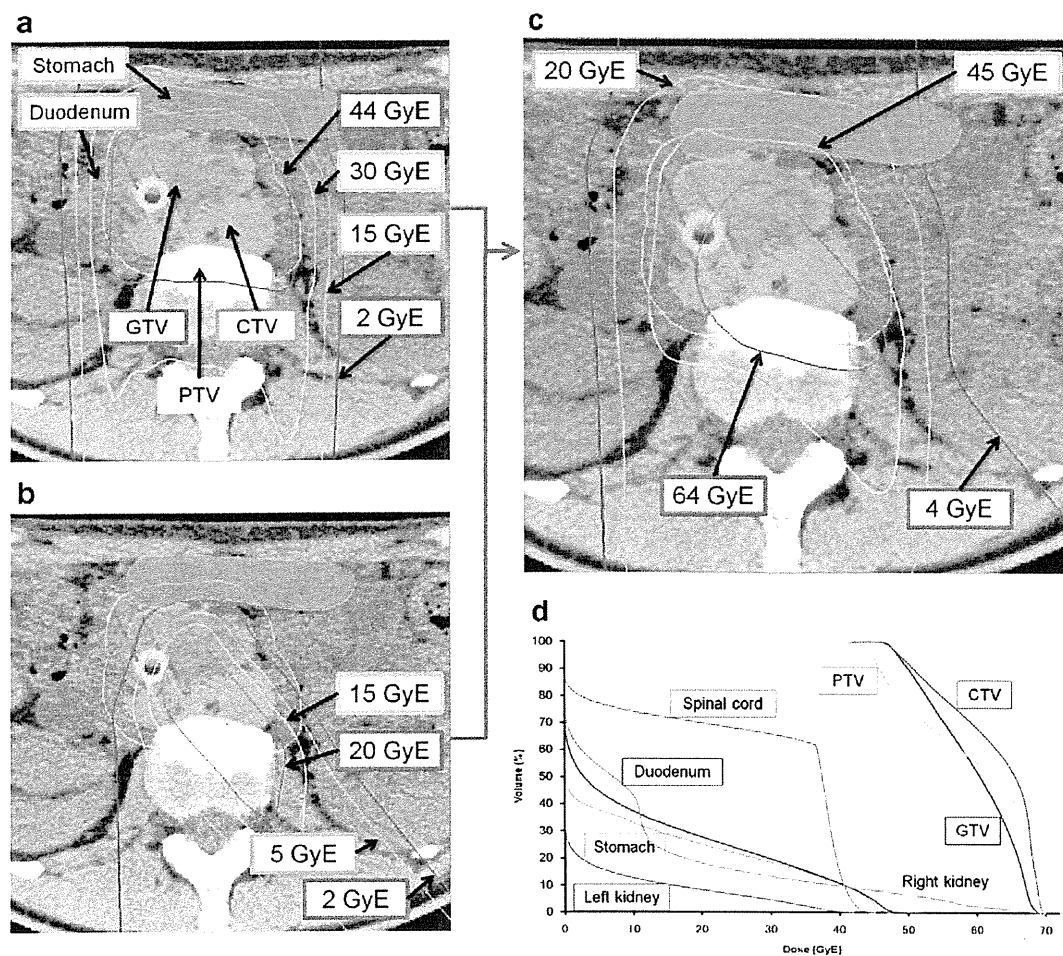


Fig. 1. A representative patient with locally advanced pancreatic cancer that was adjacent to the GI tract, treated with the gemcitabine-concurrent proton therapy (GPT) under protocol-3 (using the field-within a-field technique). (a) Dose distribution of the proton beam only at 1.8 GyE per fraction. A total dose of 45 GyE, which was the minimal dose administered to the PTV, was administered to the entire PTV. (b) Dose distribution at 0.9 GyE per fraction. A total dose of 22.5 GyE was irradiated to the PTV except for the GI tract (stomach and duodenum). (c) Summation of 1.8 GyE and 0.9 GyE in daily fractions. A total dose of 67.5 GyE was administered as the maximum dose, while the stomach and duodenum were only irradiated with approximately 45 GyE. (d) The dose-volume histogram of this plan for gross tumor volume (GTV), clinical target volume (CTV), planning target volume (PTV), and the organs-at-risk (stomach, duodenum, bilateral kidneys, and spinal cord).

1.8 GyE (total 45 GyE). With this technique, it became possible to treat all patients with the P-3 protocol alone, independent of GI-adjacency.

Follow-up

All patients received abdominal contrast-enhanced CT every three months and tumor marker monitoring every month after GPT. GIF was performed at the end of the GPT and every three months thereafter to evaluate GI toxicity. Toxicity was assessed using the Common Terminology Criteria for Adverse Events (CTCAE) v3.0.

Comparison of the protocols

To clarify the characteristics and effectiveness of the field-within-a-field technique, we analyzed the treatment plans for proton therapy using a dose-volume histogram (DVH) and compared P-3 with P-1 and P-2 in terms of $D_{80\%}$, $D_{50\%}$, and $D_{20\%}$ ($D_{x\%}$ indicates the dose delivered to $x\%$ of the target volume) of the GTV, CTV, and PTV, as well as D_{max} (a maximum dose to the target) of the stomach and duodenum.

Evaluation of local control

As the radiographic changes caused by the GPT were not significant, local control was judged comprehensively by changes in the maximum tumor diameter, the inner density on contrast-enhanced CT, the levels of tumor markers including CA19-9 and CEA, which are particularly useful for pancreatic cancer [29], and the accumulation on FDG-PET. We conclusively defined local progression as radiographic enlargement of the primary tumor or locoregional recurrence or tendency to increase in tumor markers for at least three months without any distant metastases.

End points and statistical analysis

The primary end points were feasibility and toxicity, and the secondary end points were freedom from local progression (FFLP), progression-free survival (PFS), and overall survival (OS). These were estimated from the date of the GPT initiation to the date of the event or the last follow-up.

The FFLP, PFS, and OS rates were calculated using the Kaplan-Meier method. Unpaired Student's *t*-test was used to compare parameters of dose-volume histograms between the protocols.

Statistical analyses were carried out with SPSS Version 17.0 software (SPSS, Chicago, Illinois, USA).

Role of funding source

The sponsors of the study did not play any role in the study design, data collection, data analysis, data interpretation, or writing of the report.

Results

Patient and tumor characteristics

A total of 50 eligible patients with LAPC were enrolled in this study between February 2009 and August 2010. Five patients were enrolled in P-1, 5 in P-2, and 40 in P-3. The patient characteristics are summarized in Table 1.

The analyses of proton therapy performed using the dose-volume histogram (DVH) are shown in Table 2. When compared between P-1 (for non-GI-adjacent LAPC) and P-3 using Student's *t*-test, all of the parameters, except $D_{80\%}$ of the PTV, were significantly higher in P-3 than in P-1, even though P-3 included many patients with GI-adjacent LAPC. The comparison between P-2 and P-3 did not detect any significant difference. We could not find a significant difference for D_{max} of the stomach among P-1, P-2, and P-3. While there was a possibility that bias of tumor location (all 5 patients in P-2 had tumors in the body/tail of the pancreas) and tumor size (apparently smaller in P-2 than P-3) affected to the statistical result, the mean dose of D_{max} to the duodenum in P-3 was significantly lower than in P-2. These findings support the superiority of the field-within-a-field technique.

Adjuvant chemotherapy

Among 50 patients, 45 patients (90%) were able to continue adjuvant systemic gemcitabine-based chemotherapy after GPT. Five patients (10%) failed because of unacceptable toxicity of the adjuvant chemotherapy or rapid disease progression.

Feasibility and toxicity

P-1 and P-2 protocols

All 5 patients completed the scheduled GPT in P-1. Four patients completed treatment in P-2; 1 patient (20%) could not complete proton therapy at 62.1 GyE in 23 fractions due to gastric bleeding caused by acute radiation mucositis and was cured by medication only. There was no late toxicity in that case. In P-1 and P-2, hematologic toxicities were tolerable. The acute and late toxicities in all protocols are summarized in Table 3.

P-3 protocol

Of the 40 patients in P-3, 5 patients (13%) could not receive the third gemcitabine administration because of acute hematologic and GI toxicities. The most common toxicities were neutropenia, anorexia, and weight loss (Table 3).

The major late toxicities were gastric hemorrhage and ulcer. Late gastric ulcer with hemorrhage of grade 3 or greater was observed in 4 (10%) of 40 patients. All of them had pancreatic cancer arising in the body/tail of pancreatic region. Among these 4 patients, 3 patients (8%) were cured with medication (grade 3), but 1 patient (3%) died of gastric hemorrhage six months after GPT (grade 5). This death might have been related to the GPT because gastric ulcer and erosion were confirmed by GIF on the posterior wall of the lower gastric body 2 weeks prior to death. This patient had received the maximum dose of 52 GyE to the stomach.

Local control, distant metastases and survival

The one-year FFLP, PFS, and OS rates for all patients were 81.7% (95% CI: 65–99%), 64.3% (95% CI: 48–81%), and 76.8% (95% CI: 64–89%), respectively (Figs. 2 and 3), and 79.9% (95% CI: 58–100%), 60.8% (95% CI: 41–80%), and 78.8% (95% CI: 65–93%), respectively for patients treated with P-3. Of all 50 patients, local progression developed in only 4 patients (8%), while distant metastasis developed in 15 patients (30%), within one year. Frequent sites of distant metastasis were the liver in 9 patients (18%), lung in 1 patient (2%), and the peritoneum in 3 patients (6%). Five patients (10%) were already diagnosed with liver metastases at the end of GPT. None of

Table 1
Patient characteristics.

Characteristic	Protocol P-1 (n = 5)	Protocol P-2 (n = 5)	Protocol P-3 (n = 40)
Follow-up time, months			
Median (range)	12.3 (8.2–18.6)	19.6 (17.7–21.5)	12.1 (3.2–22.3)
Age, years			
Median (range)	57 (55–75)	56 (45–72)	64 (49–83)
Gender			
Male	3	2	18
Female	2	3	22
ECOG-PS			
0	2	3	27
1	3	2	10
2	0	0	3
UICC-TNM			
T3N1M0	0	1	4
T4N0M0	1	2	6
T4N1M0	4	2	30
Tumor location			
Head	1	0	18
Body/tail	4	5	22
Tumor size, cm			
Median (range)	4.6 (3.1–5.6)	3.2 (4.5–7.2)	3.7 (2.5–7)
CEA, ng/mL			
Median (range)	3.8 (1–12)	1.6 (1–6)	3 (0.9–16.4)
CA19-9, U/mL			
Median (range)	999 (0–6010)	73.2 (15–731)	185 (0–27600)

Abbreviations: ECOG, Eastern Cooperative Oncology Group; PS, performance status; UICC-TNM, the International Union Against Cancer (UICC) TNM staging system.

Table 2
Summary of proton therapy.

	P-1 50 GyE/25 fr Median (range), GyE	P-2 70.2 GyE/26 fr Median (range), GyE	P-3 67.5 GyE/25 fr Median (range), GyE	t-test (P-1, P-3) P-value	t-test (P-2, P-3) P-value
GTV D_{80x}	49.9 (49.6–50)	58.2 (43.6–68.1)	53.4 (43.1–66.4)	<0.01	0.12
GTV D_{50x}	50.2 (50–50.4)	64.4 (49.2–70.1)	61.1 (50.2–67.6)	<0.01	0.22
GTV D_{20x}	50.6 (50.4–50.8)	66.6 (52.3–70.4)	66 (57.1–68.1)	<0.01	0.88
CTV D_{80x}	49.9 (49.4–50.4)	56.1 (41.9–65.6)	52.5 (41.7–60)	<0.01	0.19
CTV D_{50x}	50.3 (50–50.5)	64.4 (48.9–69.1)	62.6 (53.2–67.1)	<0.01	0.68
CTV D_{20x}	50.7 (50.5–51)	66.6 (51.6–70.8)	67.4 (65.4–68.2)	<0.01	0.85
PTV D_{80x}	49.7 (49.4–50.1)	51.6 (36.6–60.7)	49.4 (40.8–61)	0.72	0.42
PTV D_{50x}	50.3 (50–50.5)	61.4 (46.2–67.6)	59.5 (46.3–66.5)	<0.01	0.50
PTV D_{20x}	50.8 (50.6–51.2)	66.3 (50.8–70.4)	66.9 (63.1–68)	<0.01	0.89
Stomach D_{max}	51 (4–52)	46 (39–56)	48 (38–52)	0.52	0.54
Duodenum D_{max}	41 (40–46)	51 (51–52)	48.5 (42–52)	<0.01	<0.01

Abbreviations: GyE, gray equivalents; fr, fractions; GTV, gross tumor volume; CTV, clinical target volume; PTV, planning target volume; D_{xx} , dose delivered to x% of the target volume; D_{max} , maximum dose.

Table 3
Acute and late adverse events of grade 3 or greater.

Toxicity	P-1 (n = 5)		P-2 (n = 5)				P-3 (n = 40)							
	Acute		Acute		Late		Acute				Late			
	Grade 3		Grade 3		Grade 3		Grade 3		Grade 4		Grade 3		Grade 5	
	n	(%)	n	(%)	n	(%)	n	(%)	n	(%)	n	(%)	n	(%)
Hematologic														
Leukopenia	1	(20)	3	(60)			15	(38)	1					
Neutropenia	1	(20)	2	(40)			9	(23)	2					
Anemia			1	(20)										
Thrombocytopenia			1	(20)			2	(5)						
Gastrointestinal														
Nausea							2	(5)						
Vomiting							1	(3)						
Anorexia	1	(20)	1	(20)			3	(8)			1	(3)		
Epigastralgia	1	(20)					2	(5)						
Gastric ulcer					1	(20)					3	(8)	1	(3)
Miscellaneous														
Weight loss							3	(5)			1	(3)		
Fatigue	1	(20)					1	(3)						

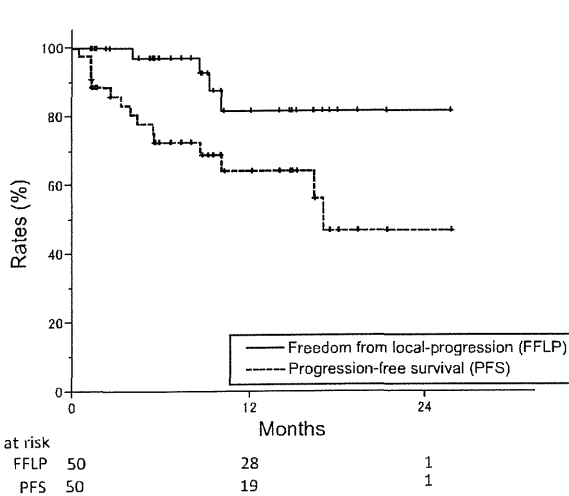


Fig. 2. The freedom from local-progression (solid line) and progression-free (dashed line) survival rates for all patients.

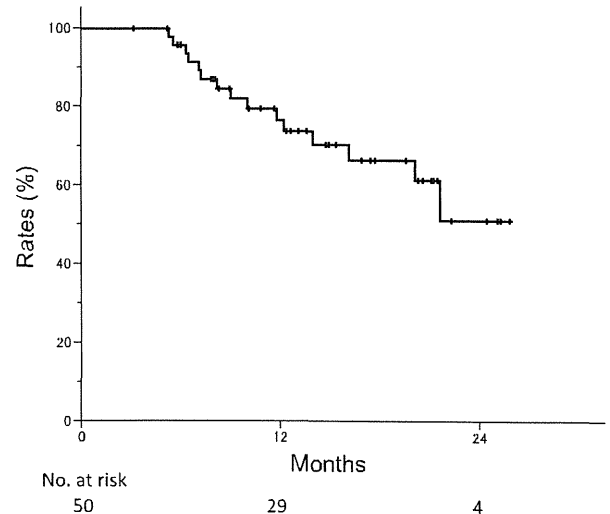


Fig. 3. The overall survival rate for all patients.

the patients died of local progression. One patient (2%) who developed both locoregional and distant metastases died of gastric hemorrhage (grade 5). Twelve patients (24%) have survived over 12 months to date without any signs of local or distant tumor progression.

Discussion

Our study indicated the high feasibility and tolerability of proton radiotherapy concurrently with high dose gemcitabine at 800 mg/m² on days 1, 8, and 15 during proton beam radiotherapy. The low frequency of grade 3 or greater acute GI toxicities, even at doses as high as 70.2 GyE (P-2) or 67.5 GyE (P-3), suggests superior dose localization of the proton beams to the target. However, late GI toxicities in P-3 (gastric ulcer and hemorrhage of grade 5) cannot be disregarded. We recognized that gastric peristalsis might bring unexpected high dose to the stomach, leading to severe complications in those patients, but it is a limitation of the current treatment planning technique. To prevent these major late toxicities, we have restricted irradiation doses to the GI tract by regulating the target fields and gantry angles and selecting an optimal split dose for the field-within-a-field technique. In contrast to the gastric toxicities, we did not encounter critical ulcer or hemorrhage in the duodenum, although it was irradiated at a dose similar to that of the stomach. The reason that no serious GI toxicity occurred in patients with pancreatic body/tail cancer seems to stem from the tolerability of the duodenum. As this lower frequency of duodenal toxicity is very interesting, we continued careful observation of the duodenum by duodenal fiberoscopy.

From our clinical experience, it appears that the field-within-a-field technique that we used at P-3 enabled us to reduce the irradiation of OAR while maintaining the necessary doses to the PTV. Our analyses of the DVH indicate that using the field-within-a-field technique can increase the dose to the PTV of patients with GI-adjacent LAPC. Despite an increase in the dose to the PTV, the maximum dose to the stomach and duodenum was not increased. In addition, the optimal split dose of the field-within-a-field technique can be selected according to the tumor adjacency to the GI tract, so that the OAR are irradiated within a tolerable limit. Accordingly, GPT performed using the field-within-a-field technique contributed to solving of the mentioned three problems: reduction of irradiation dose, gemcitabine dose, and irradiation field.

Murphy et al. demonstrated that FFLP was a significant factor of OS on multivariate analysis [20]. To improve FFLP, our GPT was designed to deliver proton beams at a higher dose to a large CTV with concurrent administration of gemcitabine. As a result, the one-year FFLP and OS rates in our study were greater than expected, with high rates of 81.7% and 76.8%, respectively. This high FFLP rate is considered to be due to a large CTV, which was locally irradiated by proton beams at a high dose; thus, a good OS rate was achieved with low toxicities. However the one-year PFS rate was 64.3% which is low compared with the high FFLP and OS rates, this PFS rate is apparently better than that of other treatment modalities for patients with LAPC. Namely, the reported PFS rates are approximately 10–20% for CRT [7,17,22] and 10–15% for gemcitabine-based chemotherapy alone [1,9]. It is likely that the substantial local control of the primary tumor exerted by GPT decreased distant metastases and that the use of concurrent and adjuvant gemcitabine has contributed to the prolongation of life of patients with LAPC.

The one-year OS rate obtained in our study is apparently better than that obtained for patients treated with chemo-photon therapy [7,17,20]. Therefore, we consider that proton therapy using the field-within-a-field technique combined with concurrent gemcitabine

or another promising chemotherapy has the potential to improve survival, including radical cure, for patients with LAPC.

Conclusions

GPT for LAPC was feasible and tolerable, and GPT using the field-within-a-field technique resulted in high FFLP and OS rates in our study. Although the number of patients enrolled in this study is too small and the follow-up periods are too short to draw any definitive conclusions, the clinical results obtained to date seem very encouraging.

Conflicts of interest

None.

References

- [1] Burris 3rd HA, Moore MJ, Andersen J, et al. Improvements in survival and clinical benefit with gemcitabine as first-line therapy for patients with advanced pancreas cancer: a randomized trial. *J Clin Oncol* 1997;15:2403–13.
- [2] Carpelan-Holmstrom M, Nordling S, Pukkala E, et al. Does anyone survive pancreatic ductal adenocarcinoma? A nationwide study re-evaluating the data of the Finnish Cancer Registry. *Gut* 2005;54:385–7.
- [3] Casper ES, Green MR, Kelsen DP, et al. Phase II trial of gemcitabine (2,2'-difluorodeoxyctidine) in patients with adenocarcinoma of the pancreas. *Invest New Drugs* 1994;12:29–34.
- [4] D'Souza MA, Shrikhande SV. Pancreatic resectional surgery: an evidence-based perspective. *J Cancer Res Ther* 2008;4:77–83.
- [5] Galloway NR, Aspe JR, Sellers C, Wall NR. Enhanced antitumor effect of combined gemcitabine and proton radiation in the treatment of pancreatic cancer. *Pancreas* 2009;38:782–90.
- [6] GITSG. Treatment of locally unresectable carcinoma of the pancreas: comparison of combined-modality therapy (chemotherapy plus radiotherapy) to chemotherapy alone. *Gastrointestinal Tumor Study Group. J Natl Cancer Inst* 1988;80:751–5.
- [7] Huang PI, Chao Y, Li CP, et al. Efficacy and factors affecting outcome of gemcitabine concurrent chemoradiotherapy in patients with locally advanced pancreatic cancer. *Int J Radiat Oncol Biol Phys* 2009;73:159–65.
- [8] Ikeda M, Okada S, Tokuyue K, Ueno H, Okusaka T. Prognostic factors in patients with locally advanced pancreatic carcinoma receiving chemoradiotherapy. *Cancer* 2001;91:490–5.
- [9] Ishii H, Furuse J, Boku N, et al. Phase II study of gemcitabine chemotherapy alone for locally advanced pancreatic carcinoma: JCOG0506. *Jpn J Clin Oncol* 2010;40:573–9.
- [10] Iwata H, Murakami M, Demizu Y, et al. High-dose proton therapy and carbon-ion therapy for stage I nonsmall cell lung cancer. *Cancer* 2010;116:2476–85.
- [11] Kagawa K, Murakami M, Hishikawa Y, et al. Preclinical biological assessment of proton and carbon ion beams at Hyogo Ion Beam Medical Center. *Int J Radiat Oncol Biol Phys* 2002;54:928–38.
- [12] Kamigaki T, Murakami M, Matsumoto IMM. A phase I study of proton beam therapy for locally advanced pancreatic cancer: analysis of feasibility and antitumor effect. *J Clin Oncol* 2008;26 [May 20 Suppl.; abstr 15675] 2008.
- [13] Kavanagh BD, Pan CC, Dawson LA, et al. Radiation dose–volume effects in the stomach and small bowel. *Int J Radiat Oncol Biol Phys* 2010;76:S101–7.
- [14] Kirkpatrick JP, van der Kogel AJ, Schultheiss TE. Radiation dose–volume effects in the spinal cord. *Int J Radiat Oncol Biol Phys* 2010;76:S42–9.
- [15] Komatsu S, Fukumoto T, Demizu Y, et al. Clinical results and risk factors of proton and carbon ion therapy for hepatocellular carcinoma. *Cancer* 2011.
- [16] Lawrence TS, Eisbruch A, McGinn CJ, Fields MT, Shewach DS. Radiosensitization by gemcitabine. *Oncology (Williston Park)* 1999;13:55–60.
- [17] Li CP, Chao Y, Chi KH, et al. Concurrent chemoradiotherapy treatment of locally advanced pancreatic cancer: gemcitabine versus 5-fluorouracil, a randomized controlled study. *Int J Radiat Oncol Biol Phys* 2003;57:98–104.
- [18] Moertel CG, Frytak S, Hahn RG, et al. Therapy of locally unresectable pancreatic carcinoma: a randomized comparison of high dose (6000 rads) radiation alone, moderate dose radiation (4000 rads + 5-fluorouracil), and high dose radiation + 5-fluorouracil: The Gastrointestinal Tumor Study Group. *Cancer* 1981;48:1705–10.
- [19] Morganti AG, Valentini V, Macchia G, et al. 5-Fluorouracil-based chemoradiation in unresectable pancreatic carcinoma: phase I-II dose-escalation study. *Int J Radiat Oncol Biol Phys* 2004;59:1454–60.
- [20] Murphy JD, Adusumilli S, Griffith KA, et al. Full-dose gemcitabine and concurrent radiotherapy for unresectable pancreatic cancer. *Int J Radiat Oncol Biol Phys* 2007;68:801–8.
- [21] Nishimura H, Ogino T, Kawashima M, et al. Proton-beam therapy for olfactory neuroblastoma. *Int J Radiat Oncol Biol Phys* 2007;68:758–62.
- [22] Okusaka T, Ito Y, Ueno H, et al. Phase II study of radiotherapy combined with gemcitabine for locally advanced pancreatic cancer. *Br J Cancer* 2004;91:673–7.

- [23] Ozaki H, Hiraoka T, Mizumoto R, et al. The prognostic significance of lymph node metastasis and intrapancreatic perineural invasion in pancreatic cancer after curative resection. *Surg Today* 1999;29:16–22.
- [24] Loehrer PJ, Powell ME, Cardenes HR, Wagner L, Brell JM, Ramanathan RK, et al. Eastern Cooperative Oncology Group. A randomized phase III study of gemcitabine in combination with radiation therapy versus gemcitabine alone in patients with localized, unresectable pancreatic cancer: E4201. *J Clin Oncol* 2008;26 [May 20 Suppl.]: abstr 4506.
- [25] Schulz-Ertner D, Tsujii H. Particle radiation therapy using proton and heavier ion beams. *J Clin Oncol* 2007;25:953–64.
- [26] Shinchi H, Takao S, Noma H, et al. Length and quality of survival after external-beam radiotherapy with concurrent continuous 5-fluorouracil infusion for locally unresectable pancreatic cancer. *Int J Radiat Oncol Biol Phys* 2002;53:146–50.
- [27] Sohn TA, Yeo CJ, Cameron JL, et al. Resected adenocarcinoma of the pancreas-616 patients: results, outcomes, and prognostic indicators. *J Gastrointest Surg* 2000;4:567–79.
- [28] Vincent A, Herman J, Schulick R, Hruban RH, Goggins M. Pancreatic cancer. *Lancet* 2011;378:607–20.
- [29] Wong D, Ko AH, Hwang J, Venook AP, Bergsland EK, Tempero MA. Serum CA19-9 decline compared to radiographic response as a surrogate for clinical outcomes in patients with metastatic pancreatic cancer receiving chemotherapy. *Pancreas* 2008;37:269–74.

Utility of Contrast-Enhanced FDG-PET/CT in the Clinical Management of Pancreatic Cancer

Impact on Diagnosis, Staging, Evaluation of Treatment Response, and Detection of Recurrence

Akinori Asagi, MD,* Koji Ohta, MD, PhD,† Junichirou Nasu, MD, PhD,* Minoru Tanada, MD,† Seijin Nadano, MD,* Rieko Nishimura, MD, PhD,‡ Norihiro Teramoto, MD, PhD,‡ Kazuhide Yamamoto, MD, PhD,§ Takeshi Inoue, MD, PhD,|| and Haruo Iguchi, MD, PhD*

Objectives: Fluorodeoxyglucose (FDG)-positron emission tomography/contrast-enhanced computed tomography (PET/CE-CT) involving whole-body scanning first by non-CE-CT and FDG-PET followed by CE-CT has been used for detailed examination of pancreatic lesions. We evaluated PET/CE-CT images with regard to differential diagnosis, staging, treatment response, and postoperative recurrence in pancreatic cancer.

Methods: Positron emission tomography/CE-CT was conducted in 108 patients with pancreatic cancer and in 41 patients with other pancreatic tumor diseases.

Results: The maximum standardized uptake value (SUV_{max}) overlapped in benign and malignant cases, suggesting that differential diagnosis of pancreatic tumors based on the SUV_{max} is difficult. In the evaluation of staging in 31 resectable pancreatic cancer by PET/CE-CT, the diagnostic accuracy rate was more than 80% for most factors concerning local invasion and 94% for distant metastasis but only 42% for lymph node metastasis. Significant positive correlations were found between the SUV_{max} and tumor size/markers, suggesting that SUV_{max} may be a useful indicator for the treatment response. Regarding the diagnosis of the postoperative recurrence, PET/CE-CT correctly detected local recurrence in all the 11 cases of recurrence, whereas abdominal CE-CT detected only 7 of 11 cases, suggesting that PET/CE-CT is superior in this context.

Conclusions: Positron emission tomography/CE-CT is useful for the clinical management of pancreatic cancer.

Key Words: contrast-enhanced PET/CT, differential diagnosis, clinical management, pancreatic cancer

(*Pancreas* 2013;42: 11–19)

Despite recent significant advances in cancer diagnosis and treatment, pancreatic cancer patients still have a very poor prognosis.¹ In Japan, the number of pancreatic cancer patients in 2002 was 21,386, whereas the number of pancreatic cancer-related deaths in 2006 was 23,366,² indicating that the number

of patients with pancreatic cancer was almost equal to the number of pancreatic cancer-related deaths. However, a slight improvement in survival has been observed with the introduction of gemcitabine and S-1 as chemotherapeutic medications for pancreatic cancer.^{3,4} Given this situation, clinical practice guidelines for pancreatic cancer have recently been established in Japan, and treatment regimens are determined on the basis of the extent of pancreatic cancer, which is evaluated by imaging. Contrast-enhanced abdominal CT (abdominal CE-CT) has primarily been used to determine the extent of pancreatic cancer.⁵ However, imaging diagnosis is also essential in the postoperative monitoring of pancreatic cancers, which often recur soon after surgery; abdominal CE-CT imaging has also been used for this purpose.

Positron emission tomography (PET), a new imaging modality, has recently been introduced in daily clinical practice, but functional imaging by PET alone does not have much diagnostic significance.⁶ Acquisition of consecutive PET and CT (PET/CT) images in addition to combination of functional PET and anatomical CT images dramatically enhances the usefulness of PET as an imaging modality.⁷ We have been using PET/CT (Aquiduo 16; Toshiba, Otawara, Japan) since the introduction of this technique at the Shikoku Cancer Center in April 2006; the CT apparatus has been dedicated to dynamic studies (contrast-enhanced PET/CT [PET/CE-CT]) on the development of this technique as a key imaging modality in the diagnosis and follow-up examinations of patients with pancreatic cancer. In this study, we retrospectively compared PET/CE-CT and abdominal CE-CT, which has been used as the primary imaging modality for the diagnosis and management of pancreatic cancer, and evaluated the efficacy of these modalities for the following functions: differential diagnosis of benign and malignant pancreatic lesions, evaluation of the extent of invasive pancreatic ductal cancer, assessment of treatment effects, and diagnosis of postoperative recurrence.

MATERIALS AND METHODS

Subjects

Positron emission tomography/CE-CT imaging technology was used to determine the extent of invasive pancreatic ductal cancer in 108 patients (64 men and 44 women, aged 45–86 years). The extent of cancer was determined according to the *Classification of Pancreatic Carcinoma, Fifth Edition* (edited by the Japan Pancreas Society [JPS]).⁸ Among the 108 subjects, operations were performed on 29 patients with locally advanced pancreatic ductal cancer, and histologic diagnosis was proven in these patients. The remaining patients were diagnosed on the basis of PET/CE-CT imaging findings and serum tumor marker values.

From the Departments of *Gastroenterology, †Gastroenterological Surgery, and ‡Pathology, Shikoku Cancer Center, Ehime; §Department of Gastroenterology and Hepatology, Okayama University Graduate School of Medicine, Okayama; and ||Department of Diagnostic Radiology, Shikoku Cancer Center, Ehime, Japan.

Received for publication May 25, 2011; accepted March 5, 2012.

Reprints: Haruo Iguchi, MD, PhD, Department of Gastroenterology, Shikoku Cancer Center, Minami-Umemotomachi Ko 160, Matsuyama, Ehime 791-0280, Japan (e-mail: higuchi@shikoku-cc.go.jp).

The authors declare no conflict of interest.

This work was supported in part by a Grant-in-Aid for Research on Applying Health Technology (grant no. H23-Cancer-General-010) from the Ministry of Health, Labor, and Welfare of Japan and Management Expenses Grants (grant no. 22-54) from the Japanese government to the National Cancer Center.

Copyright © 2012 by Lippincott Williams & Wilkins

Positron emission tomography/CE-CT imaging was conducted for relevant pancreatic tumor lesions to assess the usefulness of the maximum standardized uptake value (SUV_{max}) in differentiating benign and malignant pancreatic lesions. The SUV_{max} was the value obtained at 90 minutes after intravenous injection of fluorodeoxyglucose (FDG) in subjects with blood glucose levels of 200 mg/dL or less at the time of FDG administration.

Differential diagnosis for malignant and benign pancreatic disorders by PET/CE-CT imaging was performed in 21 patients with intraductal papillary mucinous neoplasm (IPMN; 9 men and 12 women, aged 47–78 years), in 10 patients with endocrine tumors of the pancreas (2 men and 8 women, aged 42–78 years), and in 10 patients with tumor-forming pancreatitis (chronic pancreatitis [CP] or autoimmune pancreatitis [AIP]; 8 men and 2 women, aged 40–79 years) in addition to the 108 patients with invasive pancreatic ductal cancer. Among the 21 patients with IPMN, 8 patients underwent operations, and the diagnosis of malignant tumors (intraductal papillary mucinous carcinoma [IPMC]) and benign tumors (intraductal papillary mucinous adenoma [IPMA]) was histologically proven in these patients. The remaining 13 patients were diagnosed with benign tumors (IPMA) based on the findings from imaging studies (PET/CE-CT, magnetic resonance imaging, and ultrasound), including branch type, lack of internal structures, and lack of FDG uptake. These patients are currently being observed by follow-up at more than 1 year after diagnosis. Ten patients with endocrine tumors of the pancreas were diagnosed based on the presence of hypervascular tumors with FDG accumulation on PET/CE-CT imaging. Among these patients, 7 underwent operations, and biopsies were performed in the remaining 3 patients, resulting in histologically proven diagnoses for all 10 patients. Malignancy and benignancy were determined based on histologic findings and by taking into account the presence or absence of metastatic lesions on the images. Chronic pancreatitis and AIP were diagnosed using PET/CE-CT imaging and serum levels of pancreatic enzymes and/or IgG4 according to the Diagnostic Criteria for Chronic Pancreatitis⁹ 2002 and the Diagnostic Criteria for Autoimmune Pancreatitis 2006 (JPS).¹⁰

Classification of Pancreatic Cancer

In this study, we used the classification system for pancreatic cancer defined by the JPS.⁸ According to the JPS classification system, the extent of invasive pancreatic ductal cancer was determined by taking into account local spread (T), lymph node metastases (N), and distant metastases (M). The T category was defined through determination of the presence and extent of local invasion of the pancreas and adjacent structures. Within this category, 8 local extension factors were considered: the distal bile duct (CH), duodenum (DU), serosa (S), retropancreatic tissue (RP), portal vein system (PV), arterial system (A), extrapancreatic nerve plexus (PL), and other organs (OO). The N category (lymph node metastases) was divided into 4 categories (N0–N3) according to whether metastasis was present in lymph nodes with groups 1 to 3. The presence of distant metastatic lesions, including metastasis to distant organs, the peritoneum, and group 3 lymph nodes, were defined as M1. On the basis of the grading for T, N, and M categories, tumor stage was divided into 5 groups, as shown in Fig. 1. A detailed description of stage grouping by JPS guidelines is described in a previous report by Isaji et al.⁸

PET/CT Imaging Protocol

All FDG-PET/CT studies were performed using an Aquiduo PET/CT scanner (Toshiba), which is a hybrid PET

	M0			M1	
	N0	N1	N2	N3	
T1	I	II	III	IVb	
T2	II	III	III		
T3	III	III	IVa		
T4	IVa				

FIGURE 1. Stage grouping of pancreatic cancers according to JPS guidelines.⁸ Stages of pancreatic cancer are grouped into 5 categories according to the cancer extent based on the grading of T, N, and M factors.

and 16-multidetector CT scanner. Patients fasted for at least 4 hours before the PET/CT examination. In all patients, blood glucose levels were checked before injection of the radiopharmaceutical. Intravenous injection of 3.0 MBq/kg body weight of FDG was followed by a 10-mL normal saline flush. Patients rested for approximately 90 minutes, during which time they were asked to drink 500 mL of a Japanese tea containing 5 mL of oral contrast medium (Gastrografin; Bayer Schering Pharma, Leverkusen, Germany) before image acquisition and to void before being positioned supine on the scanner table. Non-contrast-enhanced CT was performed first, from the vertex of the skull through the mid thigh at 80 to 200 mA s, 120 kV (peak) (kV[p]), and 2.0-mm collimation. Images were reconstructed as contiguous 4-mm slices. Positron emission tomography was performed immediately after non-contrast-enhanced CT without repositioning the patient. Positron emission tomography images were obtained at 7 to 8 stations per patient, with an acquisition time of 2 to 3 minutes per station, from the skull vertex through the mid thigh. The non-contrast-enhanced CT data were used for attenuation correction of PET emission images, which were coregistered with the non-contrast-enhanced CT data set. Then, dual-phase CE-CT was performed. Arterial-phase CT images were obtained 35 seconds after injection of 100 mL of iopamidol (Iopamiron 300; Bayer Schering Pharma). Contrast material was injected at 3 mL/s using a powder injector (Dual Shot GV; Nemoto, Tokyo, Japan). Arterial-phase images were obtained from the dome of the diaphragm to the iliac crest at 80 to 200 mA s, 120 kV(p), and 1.0-mm collimation. Arterial-phase images were reconstructed as contiguous 2-mm slices. Portal venous phase images were acquired after a delay of 90 seconds from the vertex of the skull through the mid thigh at 80 to 200 mA s, 120 kV(p), and 2.0-mm collimation. Portal venous phase images were reconstructed as contiguous 2-mm slices.

Positron emission tomography/CT imaging using this protocol (PET/CE-CT) can cover all angles of the diagnosis, including diagnosis of existing tumors, qualitative diagnosis, local diagnosis, and metastasis detection.

Evaluation of the Extent of Invasive Pancreatic Ductal Cancer

Operations were performed on 29 patients with locally advanced pancreatic ductal cancer (stage IVa), and diagnoses were histologically proven in these patients. Postoperatively, findings from PET/CE-CT imaging of the preoperative cancer were compared with the histologic findings of the resected specimens to determine the diagnostic accuracy rate of PET/CE-CT imaging for the evaluation of the extent of cancer progression. The degree of preoperative and postoperative cancer progression

was determined according to the JPS classification system.⁸ In another 4 patients with invasive pancreatic ductal cancer, whose preoperative stage was diagnosed as resectable IVa by PET/CE-CT, only metastatic tissue biopsies were performed because distant metastases were found after initiation of the surgical procedure (lymph node [N3], 2 cases; liver, 1 case; peritoneum, 1 case). Thus, N and M categories were examined in 31 patients with stage IVa after the addition of these 2 cases. We also compared the diagnostic accuracy rate of PET/CE-CT imaging with that of abdominal CE-CT imaging, which was extracted from the PET/CE-CT imaging, for evaluating the extent of cancer.

We further evaluated the diagnostic accuracy rate of PET/CE-CT for M factor analysis in 65 patients with stage IVb unresectable pancreatic cancer because distant metastases are not normally found in stage IVa resectable pancreatic cancer, and compared it with that of CE-CT images, which were extracted from the PET/CE-CT images. In this analysis, the reference standard for the presence of distant metastases was based on multimodality images and follow-up observations because distant metastases were not histologically proven.

To compare the diagnostic accuracy rates of PET/CE-CT and abdominal CE-CT in the context of evaluating T, N, and M factors, 2 radiologists were asked to analyze sections from these images independently, without knowledge of the results of the other imaging. If a disagreement occurred, a final decision was made after a discussion of the radiologists' analyses.

Assessment of Treatment Effects

The effects of treatment were evaluated over time in 8 patients who had undergone chemotherapy or chemoradiotherapy for unresectable locally advanced pancreatic cancer, diagnosed using PET/CE-CT imaging (tumor diameter determined by CT and SUV_{max} determined by PET) and serum tumor marker levels (CA 19-9). After determining the rate of increases and decreases in tumor diameter, SUV_{max} values and CA 19-9 levels were assessed, and correlations among these factors were examined. This analysis was conducted only on patients whose pancreatic cancer was locally confined during the ongoing treatment and was discontinued whenever distant metastasis occurred. At each evaluation of treatment effectiveness, the change rate of each variable was calculated and examined for correlations. Therefore, although 8 patients were analyzed, the number of analyzable events was 12 because multiple events occurred per case.

Diagnosis of Postoperative Recurrence

Although pancreatic cancer often recurs soon after surgery, the anatomical positional relationship between various abdominal organs may be changed by surgery; therefore, an abdominal CE-CT scan alone is often insufficient for diagnosis of local recurrence, not to mention distant metastasis. In the present study, PET/CE-CT images were used to show postoperative recurrence in 11 patients and a lack of postoperative recurrence of invasive pancreatic ductal cancer in 6 patients. Local recurrence was diagnosed by PET/CE-CT based on the findings of soft tissue density mass with FDG accumulation, whereas soft tissue density mass without FDG accumulation was diagnosed as a postoperative change. The diagnosis of local recurrence by abdominal CE-CT, on the other hand, requires not only the presence of soft tissue density mass but also the ability to compare the mass with the size with the previously measured mass. Thus, an increase in the size of the soft tissue density mass was considered a local recurrence, whereas no increase and/or little increase in size were considered a lack of local recurrence.

However, there are no standard criteria defining the increase in size that would constitute a local recurrence; thus, the diagnosis of local recurrence depends on the radiologist. In our cancer center, PET/CE-CT is usually conducted on patients in whom the serum levels of tumor markers are elevated during the follow-up period. To determine the diagnostic accuracy rate of abdominal CE-CT for the evaluation of local recurrence, 2 radiologists were asked to read only sections from abdominal CE-CT scans extracted from PET/CE-CT imaging independently, without knowledge of the results of other imaging findings. If a disagreement occurred, a final decision was made after discussion between the radiologists. Then, the diagnostic accuracy rate for local recurrence was compared between PET/CE-CT and abdominal CE-CT imaging. Although local recurrences were not histologically proven, they were confirmed by follow-up observations after the initial diagnosis by PET/CE-CT. As a result, the diagnostic accuracy rate of PET/CE-CT was 100%.

Statistical Analysis

Differences between the SUV_{max} values in various pancreatic disorders with tumorous lesions were evaluated using the *t* test. Differences in the diagnostic accuracy rates of the tested imaging modalities (PET/CE-CT and abdominal CE-CT) were evaluated using the Cochran Q test. Relationships between changes in tumor size (Ts), SUV_{max} values, and serum CA 19-9 levels during treatment were evaluated using linear regression analysis. $P < 0.05$ was considered statistically significant.

RESULTS

Differential Diagnosis of the Malignancy and Benignity of Pancreatic Lesions by PET/CE-CT Imaging

Fig. 2 shows the SUV_{max} of various pancreatic tumor diseases. The SUV_{max} (mean [SD]) of invasive pancreatic ductal cancer was 6.14 (3.51) in stages I to III, 6.28 (2.91) in stage IVa, and 7.22 (2.65) in stage IVb; thus, the values for different stages were not significantly different. However, the SUV_{max} of invasive

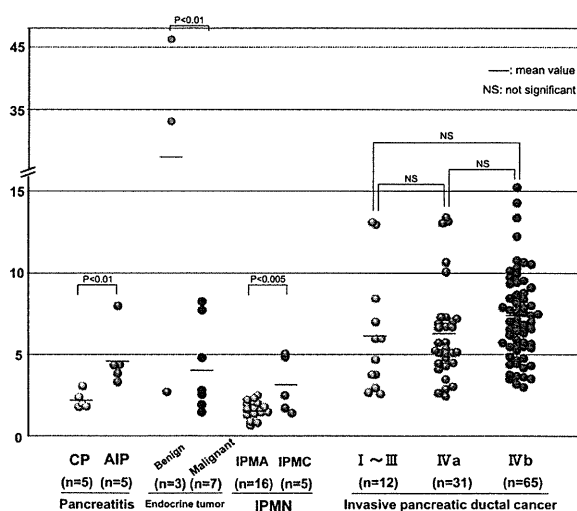


FIGURE 2. The SUV_{max} of different pancreatic tumor lesions. Ninety minutes after FDG infusion in various pancreatic tumor cases, PET/CE-CT scans were obtained to determine the SUV_{max} . Patients with blood glucose levels of 200 mg/dL or less at the time of FDG infusion were evaluated.

pancreatic ductal cancer tended to be higher than those of other pancreatic tumor diseases, excluding benign pancreatic endocrine tumors. In the case of IPMN, the SUV_{max} values (mean [SD]) were 3.09 (1.53) for IPMC (n = 5) and 1.59 (0.52) for IPMA (n = 16). The SUV_{max} of IPMC was significantly higher than that of IPMA ($P < 0.005$). In the case of pancreatic endocrine tumors, the SUV_{max} values (mean [SD]) were 27.4 (18.2) in benign cases (n = 3) and 4.21 (2.56) in malignant cases (n = 7); thus, the SUV_{was} markedly higher in benign cases. Among 3 cases of benign endocrine tumors, 2 cases exhibited extremely high SUV_{max} values, 33.5 and 46.1, and the histologic diagnosis for these cases was well-differentiated endocrine tumor with uncertain behavior according to the World Health Organization's classification of endocrine tumors published in 2004.¹¹ These 2 cases have been followed up for more than 3 years, and recurrence was not noted until August 2011. In tumor-forming chronic pancreatitis (n = 5) and tumor-forming AIP (n = 5), SUV_{max} values (mean [SD]) were 2.19 (0.48) and 4.76 (1.64), respectively; therefore, the SUV_{max} of AIP was significantly higher than that of chronic pancreatitis ($P < 0.01$).

Diagnostic Accuracy Rate of PET/CE-CT Imaging for Determining the Extent of Invasive Pancreatic Ductal Cancer

The diagnostic accuracy rate of PET/CE-CT for T, N, and M factor in patients with stage IVa resectable pancreatic cancer is shown in Table 1.

With respect to the T factor, the diagnostic accuracy rate of PET/CE-CT imaging for Ts, S, and RP was below 80%, although it was greater than 80% for CH, DU, PV, A, PL, and OO. Among these factors in the T category, A, PV, and PL are important to determine whether the locally advanced pancreatic cancer (stage IVa) is resectable. The diagnostic accuracy rates of A, PV, and PL were 97%, 86%, and 83%, respectively. Evaluation of the T factor by PET/CE-CT was based on the findings of the CE-CT images; therefore, the diagnostic accuracy rate of

PET/CE-CT for the T factor was identical to that of abdominal CE-CT (data not shown).

Abdominal CE-CT imaging was used to determine the extent of N factor based on the shape and size of lymph nodes, whereas FDG uptake was used as an additional evaluation element in PET/CE-CT imaging (Fig. 3). The accuracy rate of PET/CE-CT for the N factor was 42% (Table 1A), whereas that of abdominal CE-CT was 35% in 31 patients with stage IVa resectable pancreatic cancer (data not shown). The breakdown of differentially diagnosed N factor characteristics as measured by PET/CE-CT and histologic examination (n = 18) is shown in Table 1B. Among these N factor diagnoses, overestimation and underestimation of the extent of N factor characteristics by PET/CE-CT were observed in 6 and 12 patients, respectively. In the 6 cases of overestimation, 4 were determined to be stage IVb unresectable cases solely based on the preoperative evaluation of N2 or N3 by PET/CE-CT. In the 12 cases of underestimation, on the other hand, 9 with peripancreatic lymph node metastasis in the resected specimen, which is histologically diagnosed as N1, were included.

With respect to the M factor, the diagnostic accuracy rate of PET/CE-CT imaging was 94% in 31 patients with stage IVa resectable pancreatic cancer (Table 1A). Two metastatic cases, one with metastasis to the surface of the liver and the other with miliary nodules of peritoneal dissemination, were not detected by the preoperative PET/CE-CT. We also evaluated the diagnostic accuracy rate of PET/CE-CT for M factor characteristics in 65 patients with stage IVb unresectable pancreatic cancer (Table 2). Lymph node metastasis (N3), hepatic metastasis, and peritoneal dissemination, which are often observed as distant metastasis of pancreatic cancer, were detected in 51%, 55%, and 53% of patients by PET/CE-CT and 45%, 53%, and 31% of cases by abdominal CE-CT, respectively. The detection rates of abdominal CE-CT for lymph node metastasis (N3) and peritoneal dissemination were significantly lower than that of PET/CE-CT, although the detection rate of hepatic metastasis was

TABLE 1. (A) Diagnostic Accuracy Rate of PET/CE-CT Imaging in Determining the Extent of Cancer in 31 Patients With Preoperative Stage IVa Resectable Pancreatic Cancer and (B) Breakdown of the Differently Diagnosed Extent of the N Factor With PET/CE-CT Imaging and Histologic Examination in 18 of 31 Patients With Preoperative Stage IVa Resectable Pancreatic Cancer

(A) PET/CE-CT*	(B) Extent of N Factor		
	PET/CT Imaging	Histologic Examination	No. Cases (n = 18)
T factor	N3, N2	→N1	4
Ts	N1	→N0	2
CH	N0	→N1	9
DU	N0	→N2	1
S	N0	→N3	2
RP			
PV			
A			
PL			
OO			
N factor			
M factor			

*The extent of cancer was determined with regard to local spread (T), lymph node metastasis (N), and distant metastasis (M) according to the classification guidelines for pancreatic carcinomas published by the JPS.⁸ Preoperative cancer extent diagnosed by PET/CE-CT imaging and histologic examination of resected specimens were compared among 29 patients with stage IVa resectable pancreatic cancer to calculate the diagnostic accuracy rate of PET/CE-CT imaging. Ts was not assessable in 1 resected specimen; therefore, Ts was determined in 28 specimens. Distant metastases were histologically proven in 4 more cases (2 lymph node [N3], 1 hepatic, and 1 peritoneal metastasis), in addition to 29 patients with stage IVa resectable pancreatic cancer, in whom only tissue biopsies were performed after initiation of the surgical procedure. These 4 cases were included in N and M factor evaluation; therefore, N and M factors were histologically determined in 31 specimens.

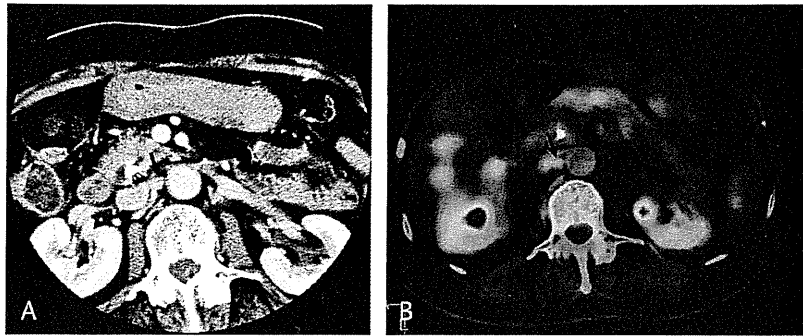


FIGURE 3. Positron emission tomography/CE-CT findings of a typical case (86-year-old woman) with lymph node metastasis. The CE-CT image shows no. 16b1 lymph node swelling (10.5 × 5.0 mm, flat shape); however, lymph node metastasis was ruled out based on the size and shape of the swelling as determined by CT (A). The PET/CT image, on the other hand, shows abnormal FDG uptake (SUV_{max} , 2.61) corresponding to this lymph node (B), suggesting lymph node metastasis. Histologic examination of the surgical specimen proved the involvement of lymph node lesions.

similar between the 2 methods. Lung and bone metastasis have rarely been detected by abdominal CE-CT because this type of imaging scans only a segmental area. Positron emission tomography/CE-CT imaging, on the other hand, scans the whole body, resulting in higher detection rates of lung and bone metastases (Table 2).

Assessment of Treatment Effects by PET/CE-CT Imaging

Unresectable pancreatic cancer is treated with chemotherapy or chemoradiotherapy, and the effectiveness of treatment is assessed according to RECIST guidelines¹² by determining the longest diameter of the measurable lesion, which is usually measured using abdominal CE-CT, and levels of serum tumor marker.

We determined the increase/decrease ratios of Ts, CA 19-9 levels, and SUV_{max} in the progressive disease and partial response groups. In contrast to small changes in Ts, the changes in CA 19-9 levels and SUV_{max} values were larger, and the patterns of changes in these indicators were similar (Fig. 4A). Among these 3 indicators, a significant positive correlation was found between SUV_{max} and CA 19-9 levels ($P < 0.0001$) and between

SUV_{max} and Ts ($P < 0.05$), but no significant correlation was found between CA 19-9 levels and Ts (Fig. 4B).

Diagnosis of Postoperative Recurrence

In patients with pancreatic cancer, recurrence is frequently observed shortly after the operation¹³; thus, diagnosis of recurrence is crucial for starting an appropriate treatment. Abdominal CE-CT is generally used for this diagnosis; however, in some cases, local recurrence may be difficult to detect because of postoperative alterations in the anatomical positions of visceral organs.^{14,15} Therefore, we compared the rates of postoperative local recurrences diagnosed by abdominal CE-CT and PET/CE-CT imaging. Abdominal CE-CT detected 7 of the 11 cases diagnosed by PET/CE-CT imaging, and in 6 cases diagnosed as not having local recurrence by PET/CE-CT imaging, 5 cases were diagnosed correctly by abdominal CE-CT (Table 3). Typical findings from imaging of local recurrences by PET/CE-CT are shown in Fig. 5.

DISCUSSION

Preoperative evaluation of the extent of pancreatic cancer is important in deciding treatment options, and abdominal CE-CT is usually used for this purpose. In the present study, we determined the diagnostic accuracy rate of PET/CE-CT in evaluating the extent of pancreatic cancer and compared it to that of abdominal CE-CT. The accuracy rate for diagnosing the T factor, which includes an evaluation of local spread or invasion into the area surrounding the pancreas, was less than 80% for Ts, S, and RP and greater than 80% for the CH, DU, PV, A, PL, and OO. Among these factors, PV, A, and PL are important in deciding whether the tumors are resectable or not, and the accuracy rates of PET/CE-CT for these factors (PV, 86%; A, 97%; and PL, 87%) were satisfactory. The accuracy rate of abdominal CE-CT imaging for the T factor was identical to that of PET/CE-CT imaging because the CE-CT portion is the main evaluation tool for T factor analysis even on PET/CE-CT imaging. With respect to the N factor, Higashi et al¹⁶ reported that the diagnostic accuracy rate assessed by CT images was not satisfactory. Zimny et al¹⁷ reported a low accuracy rate for FDG-PET in evaluation of the N factor as well. In the present study, the diagnostic accuracy rate of PET/CE-CT for the N factor was 42%, despite the fact that the diagnosis was based on both CT images of the size and shape of lymph nodes and FDG uptake on PET, whereas the diagnostic accuracy rate of abdominal CE-CT was even

TABLE 2. Difference Between PET/CE-CT and Abdominal CE-CT in the Diagnosis of the Extent of M Factor Progression in 65 Patients With Stage IVb Unresectable Pancreatic Cancer

	PET/CE-CT	Abdominal CE-CT
Lymph node (N3)	33 (51%)	29 (45%)*
Liver	36 (55%)	35 (53%)
Peritoneum	35 (53%)	20 (31%)†
Lung	12 (18%)	5 (8%)†
Bone	16 (24%)	3 (5%)†

Positron emission tomography/CE-CT was conducted at the time of diagnosis in 65 patients. The portions that correspond to the abdominal CE-CT were extracted from the PET/CE-CT images and reconstructed. Then, 2 radiologists assessed the extent of M factor characteristics on these extracted images. If a disagreement occurred, a final decision was made after discussion between the radiologists.

* $P < 0.05$ versus PET/CE-CT.

† $P < 0.01$ versus PET/CE-CT.

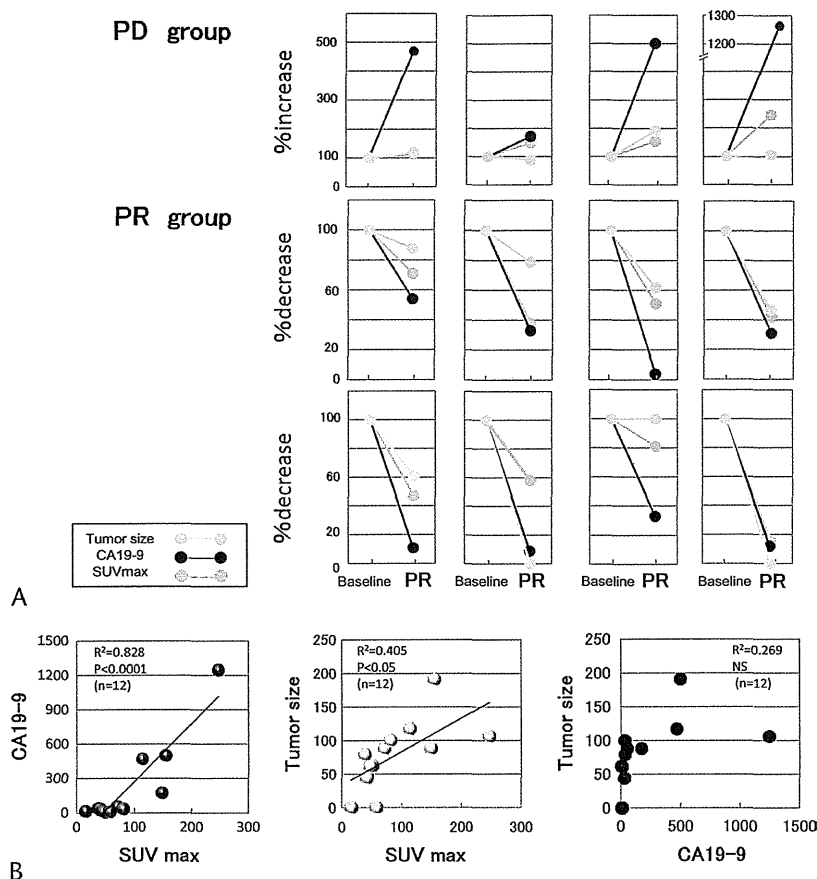


FIGURE 4. Monitoring treatment effectiveness in invasive pancreatic ductal cancer by PET/CE-CT. Chemotherapy or chemoradiotherapy was conducted in 8 patients with unresectable locally advanced pancreatic cancer. Positron emission tomography/CE-CT imaging (SUV_{max} by PET and T_s by CE-CT) and levels of serum tumor markers (CA 19-9) were used to assess the effects of treatment over time. Only tumors that were found to be locally confined during treatment were analyzed. Cases in which distant metastasis occurred were excluded from analysis. A, Changes in T_s, CA 19-9, and SUV_{max} during treatment. Compared with the baseline values (100%), the values at partial response or progressive disease are indicated by the percent decrease or increase. B, Correlations between the rate of change in T_s, CA 19-9, and SUV_{max} during treatment. NS indicates not significant.

lower (35%). The extent of the N factor was differentially diagnosed with PET/CE-CT and histologic examination in 18 cases; however, of these 18 cases, 9 cases of group 1 lymph node metastasis were diagnosed as N0 on PET/CE-CT but as N1 by histologic examination. These lymph nodes were attached to the resected specimens; therefore, detection of such lymph node

metastasis by imaging seems impossible because of their small size and/or their merging with pancreatic tumors. If these 9 cases were excluded from our calculation of the diagnostic accuracy rate, the accuracy rate of PET/CE-CT for the N factor would be 13 (59%) of 22, although even this level is low. These results indicate that PET/CE-CT imaging is not very useful for assessing

TABLE 3. Positron Emission Tomography/CE-CT Versus Abdominal CE-CT for the Diagnosis of Postoperative Local Recurrence

CT		PET/CT	
		Recurrence (n = 11)	No Recurrence (n = 6)
CT	Recurrence	7	1
	No recurrence	4	5
	Accuracy rate	63%	83%

Shown are 11 cases diagnosed as “local recurrence” and 6 cases diagnosed as “no recurrence” by PET/CE-CT imaging during the postoperative monitoring period. The portion that corresponds to the abdominal CE-CT was extracted from PET/CE-CT images and reconstructed. Local recurrence was diagnosed by PET/CE-CT based on the findings of soft tissue-density mass with FDG accumulation, whereas soft tissue density mass without FDG accumulation was diagnosed as a postoperative change. The diagnosis of local recurrence by abdominal CE-CT, on the other hand, required not only the presence of soft tissue density mass but also the comparison of the current T_s with the previous measure of T_s. Two radiologists assessed local recurrence on these extracted images. If a disagreement occurred, a final decision was made after discussion between the radiologists.